Formation Control for an UAV Team with Environment-Aware Dynamic Constraints

Zhongjun Hu and Xu Jin, *Member, IEEE*

***Abstract*—State-of-the-art literature on constrained multiagent system operations can only deal with constant or at best time-varying constraint requirements. Such constraint formulations cannot respond well to the dynamic environment and presence of external agents outside of the multiagent system. In this work, we consider a formation tracking problem for a group of unmanned aerial vehicles (UAVs) in the presence of a physical attacker. The safety/performance constraint functions are environment-aware and dynamic in nature, whose formulation depends on certain path parameters and presence of the attacker. The dependence on path ensures adaptation to the dynamic operation environment. The dependence on the attacker ensures swift adjustment based on the relative distances between the attacker and agents. UAV desired paths and desired path speeds can also be both path- and attacker-dependent. Composite barrier functions have been proposed to address the constraint requirements. Neural network is used to approximate unknown attacker velocity, where the ideal weight matrix is learned by adaptive laws. Besides, unknown system parameters and external disturbances are estimated by adaptive laws. The proposed formation architecture can ensure formation tracking errors converge exponentially to small neighborhoods near the equilibrium, with all constraint requirements met. At the end a simulation study further illustrates the proposed scheme and demonstrates its efficacy.**

***Index Terms*—Environment-aware dynamic constraints, multi-agent systems, adaptive neural network control, robust formation tracking**

I. Introduction

FORMATION control of unmanned aerial vehicles (UAVs), especially quadrotors, has many practical applications in surveillance [1], [2], search and rescue [3], contour mapping [4], [5], source locating [6], object lifting and transporting [7]–[10], just to name a few.

Safety and performance constraints on motion control for multiagent systems has been rigorously studied in recent years. Violation of such requirements can lead to performance degradation and/or system damage, which can result in operation failures. Common approaches in handling constraint requirements include control barrier functions (CBFs) [11]–[14], barrier functions/barrier Lyapunov functions (BLFs) [15]–[18], and model predictive control (MPC) methods [19]–[23]. However, these algorithms can only deal with constant or at best time-varying safety constraint requirements. Constant constraints are often conservative in formulation, as control engineers have to assume worst case scenarios throughout the entire operation. Time-varying safety constraints give system designers more flexibility, yet many environmental factors, such as space- or geometry-related environment boundaries are not time-dependent. This requires the safety/performance constraints should be environment-aware in response to the complex environment.

Furthermore, in practical scenarios, external agents outside of the multiagent systems can also influence the safety and performance constraint formulations. Consider a real-world example from the nature, where a fish school faces attacks from predators. We can observe that each fish will attempt to swim as close to other fish as possible while avoiding collisions; whereas in the absence of predators, the inter-fish distances can be relaxed inside the fish school. Meanwhile, to ensure survival, each fish should not separate too far from the rest of the school. Similarly, when an "attacker" is approaching an autonomous multiagent system, the safety and performance constraints should adapt dynamically, with the desired path and desired path speed also change accordingly. This requires the safety/performance constraint should be dynamic in nature, which depend on the presence of external agents.

It is worth pointing out that the "attacker" considered here is a physical attacker, which is different from the well-studied cyber-attacks on multiagent systems in the literature, including [24]–[29]. These works have extensively examined strategies to mitigate cyber-attacks for multi-UAV systems, including deception attacks, replay attacks, denial-of-service attacks, false-data injection attacks, camouflage attacks, and actuation attacks. However, to launch such cyber-attacks on multi-agents systems often requires sophisticated skills or enormous resources, which can make such attacks not economically worthwhile from the attacker's viewpoint. Compared with cyber-attacks, the physical attacker considered in our work are non-cyber attacks that are much easier to launch and require less skills and resources from the attacker. Therefore, such attacks pose greater risks than cyber-attacks.

Our recent work [30] published in this journal proposed constrained path-following control architectures for a ground vehicle, where the constraint requirements depend on a path parameter, instead of being merely constants or time-varying. The work focuses on the spatial path following task without temporal restrictions, and hence can result in less aggressive dynamic behavior. However, our work [30] only focuses on a single vehicle operating on a two-dimensional plane, hence is not suitable for addressing multiagent UAV system operations in a 3D space. Moreover, the constraint requirements in [30] cannot respond to the presence of external agents outside of the multiagent system.

In this paper we consider a formation tracking problem for a team of UAVs in the presence of a physical attacker, where each UAV is communicating with its neighbors over an undirected topology. For the first time in the literature, we

This work was supported in part by the National Science Foundation under Grant 2131802.

Zhongjun Hu and Xu Jin are with the Department of Mechanical and Aerospace Engineering, University of Kentucky, Lexington, KY 40506, USA (E-mail: ZhongjunHu@uky.edu; xu.jin@uky.edu).

consider environment-aware dynamic constraint requirements on safety and performance. First, for the *performance constraints*, the UAV team needs to track the desired path closely under disruptions from the physical attacker. More specifically, the line-of-sight (LOS) distance between each UAV and its reference path should not be too large. Second, for the *safety constraints*, we need to guarantee that the LOS relative distance between any two UAVs cannot be either too small or too large. At the same time, the UAV team needs to avoid collision with the attacker, which can adjust velocity depending on the relative coordinates between the attacker and agents in the UAV team. Due to the complex operating environment for the UAV team, these safety and performance constraint requirements cannot be merely constant or time-varying, but instead need to depend on path parameters and the attacker. The UAV desired paths and desired path speeds are also path- and attacker-dependent. The proposed algorithm incorporates adaptive neural network control scheme to address unknown attacker velocity. Besides, unknown system parameters and uncertainties are estimated by adaptive laws. The algorithm will ensure exponential convergence of all position and attitude tracking errors, while at the same time guarantee safety and performance of the team.

Main technical novelties can be summarized as:

1. Unlike existing works on control barrier functions (CBFs) [11]–[14], barrier Lyapunov functions (BLFs) [15]–[18], and model predictive control (MPC) methods [19]–[23], which can only address constant or at best time-varying constraint requirements, in this work we consider environment-aware dynamic constraint functions that are both path- and attacker-dependent. The dependence on path ensures that constraint functions can adapt to the dynamic operation environment. The dependence on the attacker ensures that constraint functions can be dynamically adjusted, based on the relative distances between the attacker and agents.
2. We consider the UAV desired paths and desired path speeds are also path- and attacker-dependent.
3. Unlike some literature on multiagent system path following, which only incorporates one environment-related path parameter for the whole team [31]–[33], in this work each agent in the UAV team has its own path parameter, making the proposed algorithm a fully distributed one.

We will use the following standard notations in this paper. First, $\mathbb{R}$ is real number set and I_m denotes the $m \times m$ identity matrix. Moreover, $(\cdot)^{\mathrm{T}}$ is the transpose of $(\cdot)$, $|\cdot|$ represents absolute values for scalars, and $||\cdot||$ represents Euclidean norms for vectors and induced norms for matrices. Furthermore, we use $\mathrm{c}\theta$ to denote $\cos\theta$, $\mathrm{s}\theta$ to denote $\sin\theta$, and $\mathrm{t}\theta$ to denote $\tan\theta$. We also write $\dot{(\cdot)}$ as the first order time derivative of $(\cdot)$, if $(\cdot)$ is differentiable, and $\ddot{(\cdot)}$ as the second order time derivative of $(\cdot)$. Besides, for any two vectors $v_1,\ v_2 \in \mathbb{R}^3$, the cross-product operator $\mathbb{S}(\cdot)$ gives $\mathbb{S}(v_1)v_2 = v_1 \times v_2$. It is also true that $\mathbb{S}(v_1)v_2 = -\mathbb{S}(v_2)v_1$ and $v_1^{\mathrm{T}}\mathbb{S}(v_2)v_1 = 0$. Next, $\otimes$ represents the Kronecker product. In addition, for any matrix $A \in \mathbb{R}^{n\times m}$ where $A = [A_1, \cdots, A_m]$ and $A_j \in \mathbb{R}^n$, $j = 1, \cdots, m$, the vector operator $\mathrm{vec}(\cdot)$ gives $\mathrm{vec}(A) = [A_1^{\mathrm{T}}, \cdots, A_m^{\mathrm{T}}]^{\mathrm{T}} \in \mathbb{R}^{nm}$. Finally, $\mathrm{SO}(3) = \{\Omega \in \mathbb{R}^{3\times 3} \mid \Omega^{\mathrm{T}}\Omega = I_3\}$ is a set of orthogonal matrices in $\mathbb{R}^{3\times 3}$ and $\mathrm{S}^2 = \{x \in \mathbb{R}^3 \mid ||x|| = 1\}$ is a set of unit vectors in $\mathbb{R}^3$.

II. Problem formulation

A. Basic Graph Theory and Notations

A weighted undirected graph is represented by $\mathcal{G} = (\mathcal{V}, \mathcal{E})$, where $\mathcal{V} = \{1, \cdots, N\}$ is a nonempty set of nodes/agents, and $\mathcal{E} \subset \mathcal{V} \times \mathcal{V}$ is the set of edges/arcs. $(j, i) \in \mathcal{E}$ implies that agent i can receive information from its neighboring agent j, and vice versa. In this case, agent j is called a neighbor of agent i. Furthermore, $\mathcal{N}_i$ denotes the set of neighbors of agent i and $|\mathcal{N}_i|$ represents the number of neighbors. In our following controller design and stability analysis, we suppose that each agent in the group has at least one neighbor, which means that $|\mathcal{N}_i| \geq 1$ $(i = 1, \cdots, N)$. The topology of a weighted graph $\mathcal{G}$ is often represented by the adjacency matrix $\mathcal{A} = [a_{ij}] \in \mathbb{R}^{N\times N}$, where $a_{ij} = 1$ if $(j, i) \in \mathcal{E}$; otherwise $a_{ij} = 0$. It is assumed that $a_{ii} = 0$, and the topology is fixed, i.e., $\mathcal{A}$ is time invariant. Define $\bar{a}_i = \sum_{j=1}^{N} a_{ij}$ as the weighted in-degree of node i and $\bar{\mathcal{A}} = \mathrm{diag}(\bar{a}_1, \cdots, \bar{a}_N) \in \mathbb{R}^{N\times N}$ as the in-degree matrix. The graph Laplacian matrix is $\mathcal{L} = \bar{\mathcal{A}} - \mathcal{A} \in \mathbb{R}^{N\times N}$.

B. System Dynamics

We consider a group of N quadrotors $(i = 1, \cdots, N)$, where each has the following dynamics

$$m_i\ddot{p}_i(t) = -F_i(t)R(\Theta_i(t))e_z + m_i g e_z + N_{1i}(t), \quad (1)$$

$$\dot{\Theta}_i(t) = T(\Theta_i(t))\omega_i(t), \quad (2)$$

$$J_i\dot{\omega}_i(t) + \mathbb{S}(\omega_i(t))J_i\omega_i(t) = \tau_i(t) + N_{2i}(t), \quad (3)$$

where $p_i(0) = p_{i10} \in \mathbb{R}^3$, $\dot{p}_i(0) = p_{i20} \in \mathbb{R}^3$, $\Theta_i(0) = \Theta_{i0} \in \mathbb{R}^3$, $\omega_i(0) = \omega_{i0} \in \mathbb{R}^3$ are initial conditions. Moreover, $m_i \in \mathbb{R}$, $m_i > 0$ is the mass of the ith quadrotor $(i = 1, \cdots, N)$, and $J_i \in \mathbb{R}^{3\times 3}$ is a symmetric positive definite matrix representing the inertia of the ith quadrotor $(i = 1, \cdots, N)$. The position and attitude in the inertial reference frame are represented as $p_i(t) = [x_i(t),\ y_i(t),\ z_i(t)]^{\mathrm{T}} \in \mathbb{R}^3$ and $\Theta_i(t) = [\phi_i(t),\ \theta_i(t),\ \psi_i(t)]^{\mathrm{T}} \in \mathbb{R}^3$, respectively. $F_i(t) \in \mathbb{R}$ and $\tau_i(t) \in \mathbb{R}^3$ represent the thrust and torques of the ith quadrotor $(i = 1, \cdots, N)$, respectively. $N_{1i}(t) \in \mathbb{R}^3$ and $N_{2i}(t) \in \mathbb{R}^3$ denote the external disturbances. Furthermore, $g \in \mathbb{R}$ is the gravitational acceleration and $e_z = [0,\ 0,\ 1]^{\mathrm{T}} \in \mathbb{R}^3$ is a unit vector. $R(\Theta_i(t)) \in \mathrm{SO}(3)$ is a rotation matrix, which translates the translational velocity vector in the body-fixed frame into the rate of change of the position vector in the inertial frame

$$R(\Theta_i) = \begin{bmatrix} \mathrm{c}\theta_i\mathrm{c}\psi_i & \mathrm{s}\phi_i\mathrm{s}\theta_i\mathrm{c}\psi_i - \mathrm{c}\phi_i\mathrm{s}\psi_i & \mathrm{c}\phi_i\mathrm{s}\theta_i\mathrm{c}\psi_i + \mathrm{s}\phi_i\mathrm{s}\psi_i \\ \mathrm{c}\theta_i\mathrm{s}\psi_i & \mathrm{s}\phi_i\mathrm{s}\theta_i\mathrm{s}\psi_i + \mathrm{c}\phi_i\mathrm{c}\psi_i & \mathrm{c}\phi_i\mathrm{s}\theta_i\mathrm{s}\psi_i - \mathrm{s}\phi_i\mathrm{c}\psi_i \\ -\mathrm{s}\theta_i & \mathrm{s}\phi_i\mathrm{c}\theta_i & \mathrm{c}\phi_i\mathrm{c}\theta_i \end{bmatrix}. \quad (4)$$

Moreover, define a body-fixed frame with the origin being at the center of mass for each quadrotor, and the rotational velocities with respect to this body-fixed frame are denoted by $\omega_i(t) = [\omega_{xi}(t),\ \omega_{yi}(t),\ \omega_{zi}(t)]^{\mathrm{T}} \in \mathbb{R}^3$. Besides, $T(\Theta_i(t))$ is a transformation matrix that relates the angular velocity in the

This article has been accepted for publication in IEEE Transactions on Intelligent Vehicles. This is the author's version which has not been fully edited and content may change prior to final publication. Citation information: DOI 10.1109/TIV.2023.3295354

body-fixed frame to the rate of change of Euler angles in the inertial frame, and is given by

$$T(\Theta_i) = \begin{bmatrix} 1 & \mathrm{s}\phi_i \mathrm{t}\theta_i & \mathrm{c}\phi_i \mathrm{t}\theta_i \\ 0 & \mathrm{c}\phi_i & -\mathrm{s}\phi_i \\ 0 & \mathrm{s}\phi_i/\mathrm{c}\theta_i & \mathrm{c}\phi_i/\mathrm{c}\theta_i \end{bmatrix}. \tag{5}$$

As shown in Appendix A (see (57)–(61)), the rotational dynamics (2) and (3) can be rewritten as

$$\begin{aligned} &M_i(\Theta_i(t))\ddot{\Theta}_i(t) + C_i(\Theta_i(t), \dot{\Theta}_i(t))\dot{\Theta}_i(t) \\ &\quad = \Psi^{\mathrm{T}}(\Theta_i(t))J_i^{\mathrm{T}}\tau_i(t) + \Psi^{\mathrm{T}}(\Theta_i(t))J_i^{\mathrm{T}}N_{2i}(t), \end{aligned} \tag{6}$$

where $\Psi(\Theta_i(t))$, $M_i(\Theta_i(t))$, and $C_i(\Theta_i(t), \dot{\Theta}_i(t))$ are given in (57), (60), and (61), respectively.

C. Path-Following Formation with a Physical Attacker

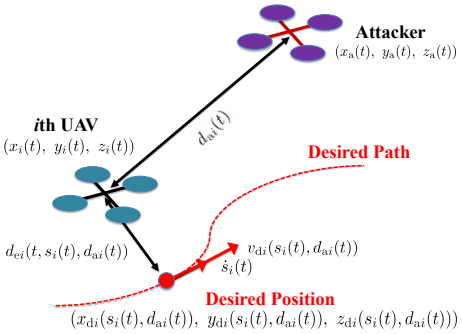

Fig. 1. A brief graphical illustration for the ith UAV ($i = 1, \cdots, N$) path following in the presence of a physical attacker.

See Figure 1 for an illustration of the ith quadrotor ($i = 1, \cdots, N$) path-following problem in the presence of a physical attacker. The LOS distance $d_{\mathrm{a}i}(t)$ between the ith quadrotor and attacker is

$$d_{\mathrm{a}i} \triangleq \sqrt{(x_i - x_{\mathrm{a}})^2 + (y_i - y_{\mathrm{a}})^2 + (z_i - z_{\mathrm{a}})^2}, \tag{7}$$

where $p_{\mathrm{a}}(t) = [x_{\mathrm{a}}(t),\ y_{\mathrm{a}}(t),\ z_{\mathrm{a}}(t)]^{\mathrm{T}}$ is the attacker position.

The desired path for the ith quadrotor ($i = 1, \cdots, N$) is denoted by $p_{\mathrm{d}i}(s_i(t), d_{\mathrm{a}i}(t)) \triangleq [x_{\mathrm{d}i}(s_i(t), d_{\mathrm{a}i}(t)),\ y_{\mathrm{d}i}(s_i(t), d_{\mathrm{a}i}(t)),\ z_{\mathrm{d}i}(s_i(t), d_{\mathrm{a}i}(t))]^{\mathrm{T}} \in \mathbb{R}^3$, where $s_i(t) \in \mathbb{R}$ is a path parameter evolving with time. As pointed out in Figure 1, $p_{\mathrm{d}i}(s_i(t), d_{\mathrm{a}i}(t))$ is any *arbitrary* point on the desired path, not necessarily the vehicle's closest/projection point on the desired path. Finally, $v_{\mathrm{d}i}(s_i(t), d_{\mathrm{a}i}(t))$ is the desired path speed associated with the path parameter $s_i(t)$ and attacker distance $d_{\mathrm{a}i}(t)$.

D. System Performance and Safety Constraints

For the ith quadrotor ($i = 1, \cdots, N$), define the LOS distance tracking error $d_{\mathrm{e}i}(t, s_i(t), d_{\mathrm{a}i}(t))$ as

$$d_{\mathrm{e}i} \triangleq \sqrt{(x_i - x_{\mathrm{d}i})^2 + (y_i - y_{\mathrm{d}i})^2 + (z_i - z_{\mathrm{d}i})^2}. \tag{8}$$

Besides, the desired LOS relative distance between ith and jth ($j \in \mathcal{N}_i$) quadrotors $L_{ij}(s_i(t), d_{\mathrm{a}i}(t), s_j(t), d_{\mathrm{a}j}(t))$ is

$$L_{ij} \triangleq \sqrt{(x_{\mathrm{d}i} - x_{\mathrm{d}j})^2 + (y_{\mathrm{d}i} - y_{\mathrm{d}j})^2 + (z_{\mathrm{d}i} - z_{\mathrm{d}j})^2}, \tag{9}$$

and the actual LOS relative distance $d_{ij}(t)$ is

$$d_{ij} \triangleq \sqrt{(x_i - x_j)^2 + (y_i - y_j)^2 + (z_i - z_j)^2}. \tag{10}$$

During the formation operation, certain system constraint requirements need to be satisfied, in order to ensure *precise* and *safe* operation. These constraints are environment-aware and dynamic in nature. First, the LOS distance tracking error for the ith quadrotor $d_{\mathrm{e}i}(t, s_i(t), d_{\mathrm{a}i}(t))$ ($i = 1, \cdots, N$) has to satisfy the following *performance constraint*

$$d_{\mathrm{e}i}(t, s_i(t), d_{\mathrm{a}i}(t)) < \Omega_{\mathrm{H}i}(s_i(t), d_{\mathrm{a}i}(t)), \tag{11}$$

where, for all $t \geq 0$, $\Omega_{\mathrm{H}i}(s_i(t), d_{\mathrm{a}i}(t)) > 0$ is the user-defined constraint requirement for the distance tracking error $d_{\mathrm{e}i}(t, s_i(t), d_{\mathrm{a}i}(t))$, and is at least three-times continuously differentiable and has bounded derivatives with respect to the path parameter $s_i(t)$ and LOS attacker distance $d_{\mathrm{a}i}(t)$. Moreover, $\Omega_{\mathrm{H}i}(s_i(t), d_{\mathrm{a}i}(t))$ is designed such that when $t = 0$, $d_{\mathrm{e}i}(0, s_i(0), d_{\mathrm{a}i}(0)) < \Omega_{\mathrm{H}i}(s_i(0), d_{\mathrm{a}i}(0))$.

It is easy to see from (8) that $d_{\mathrm{e}i}(t, s_i(t), d_{\mathrm{a}i}(t)) \geq 0$ at all time. However, in order to avoid singularity in the controller design later in the analysis, it is needed for $d_{\mathrm{e}i}(t, s_i(t), d_{\mathrm{a}i}(t))$ to be bounded away from the origin. Therefore, the constraint requirement (11) is modified as

$$0 < \varepsilon_{\mathrm{e}i} < d_{\mathrm{e}i}(t, s_i(t), d_{\mathrm{a}i}(t)) < \Omega_{\mathrm{H}i}(s_i(t), d_{\mathrm{a}i}(t)), \tag{12}$$

where $\varepsilon_{\mathrm{e}i}$ is any arbitrarily small positive number. Note that (12) is equivalent to

$$-\varepsilon_{\mathrm{e}i} < d_{\varepsilon\mathrm{e}i}(t, s_i(t), d_{\mathrm{a}i}(t)) < \Omega_{d\mathrm{H}i}(s_i(t), d_{\mathrm{a}i}(t)), \tag{13}$$

where $d_{\varepsilon\mathrm{e}i}(t, s_i(t), d_{\mathrm{a}i}(t)) \triangleq d_{\mathrm{e}i}(t, s_i(t), d_{\mathrm{a}i}(t)) - 2\varepsilon_{\mathrm{e}i}$ and $\Omega_{d\mathrm{H}i}(s_i(t), d_{\mathrm{a}i}(t)) \triangleq \Omega_{\mathrm{H}i}(s_i(t), d_{\mathrm{a}i}(t)) - 2\varepsilon_{\mathrm{e}i}$.

Remark 2.1: In the analysis to be presented later, we will show that the distance tracking error $d_{\mathrm{e}i}(t, s_i(t), d_{\mathrm{a}i}(t))$ will converge to a small neighbourhood of $2\varepsilon_{\mathrm{e}i}$, which is a shifted equilibrium point bounded away from zero. This ensures that the tracking error will decrease over time, yet stay positive at all time. This equilibrium shift method to avoid singularity in the control design is common in the literature [34]–[36]. More discussion on how the modified constraint requirement (13) can help avoid singularity in the control design can be seen in the later Remark 3.2.

Second, each quadrotor in the group needs to avoid collision with the attacker at all time. Namely, the ith quadrotor ($i = 1, \cdots, N$) needs to satisfy the following *safety constraint*

$$d_{\mathrm{a}i}(t) > \Omega_{\mathrm{a}i}(s_i(t)), \tag{14}$$

where $\Omega_{\mathrm{a}i}(s_i(t)) > 0$ is a user-defined path-dependent constraint requirement, which is designed to be at least three-times continuously differentiable and has bounded derivatives with respect to $s_i(t)$. Moreover, $\Omega_{\mathrm{a}i}(s_i(t))$ is designed such that when $t = 0$, $d_{\mathrm{a}i}(0) > \Omega_{\mathrm{a}i}(s_i(0))$.

Furthermore, define the LOS relative distance tracking error between the ith and jth quadrotors ($i = 1, \cdots, N$, $j \in \mathcal{N}_i$) as

$$\begin{aligned} &d_{\mathrm{e}ij}(t, s_i(t), d_{\mathrm{a}i}(t), s_j(t), d_{\mathrm{a}j}(t)) \\ &\quad \triangleq d_{ij}(t) - L_{ij}(s_i(t), d_{\mathrm{a}i}(t), s_j(t), d_{\mathrm{a}j}(t)), \end{aligned} \tag{15}$$

where $s_j(t) \in \mathbb{R}$ is the path parameter for the jth quadrotor and $d_{\mathrm{a}j}(t) \in \mathbb{R}$ is the LOS distance between the jth quadrotor and attacker. The following *safety constraint* needs to be met

$$\begin{aligned} d_{\mathrm{e}ij}(t, s_i(t), d_{\mathrm{a}i}(t), s_j(t), d_{\mathrm{a}j}(t)) \\ \in \big(-\Omega_{\mathrm{L}ij}(s_i(t), d_{\mathrm{a}i}(t), s_j(t), d_{\mathrm{a}j}(t)), \\ \Omega_{\mathrm{H}ij}(s_i(t), d_{\mathrm{a}i}(t), s_j(t), d_{\mathrm{a}j}(t))\big), \end{aligned} \tag{16}$$

where, for all $t \geq 0$, $\Omega_{\mathrm{H}ij}(s_i(t), d_{\mathrm{a}i}(t), s_j(t), d_{\mathrm{a}j}(t)) > 0$ is the path- and attacker-dependent higher bound for $d_{\mathrm{e}ij}(t, s_i(t), d_{\mathrm{a}i}(t), s_j(t), d_{\mathrm{a}j}(t))$, and $-\Omega_{\mathrm{L}ij}(s_i(t), d_{\mathrm{a}i}(t), s_j(t), d_{\mathrm{a}j}(t)) < 0$ is the lower bound, with $0 < \Omega_{\mathrm{L}ij}(s_i(t), d_{\mathrm{a}i}(t), s_j(t), d_{\mathrm{a}j}(t)) < L_{ij}(s_i(t), d_{\mathrm{a}i}(t), s_j(t), d_{\mathrm{a}j}(t))$. The higher and lower constraint functions are both at least three-times continuously differentiable and have bounded derivatives with respect to the path parameters $s_i(t)$ and $s_j(t)$ and LOS attacker distances $d_{\mathrm{a}i}(t)$ and $d_{\mathrm{a}j}(t)$. Moreover, the higher and lower bounds are designed such that when $t = 0$, $d_{\mathrm{e}ij}(0, s_i(0), d_{\mathrm{a}i}(0), s_j(0), d_{\mathrm{a}j}(0)) \in \big(-\Omega_{\mathrm{L}ij}(s_i(0), d_{\mathrm{a}i}(0), s_j(0), d_{\mathrm{a}j}(0)), \Omega_{\mathrm{H}ij}(s_i(0), d_{\mathrm{a}i}(0), s_j(0), d_{\mathrm{a}j}(0))\big)$. The constraint requirement (16) means that the inter-quadrotor distances cannot be either too small or too large, such that the collision avoidance and formation keeping can be ensured.

Last but not least, the attitude tracking error for the ith quadrotor ($i = 1, \cdots, N$) is defined as

$$z_{\Theta i}(t) = [z_{\phi i}(t),\ z_{\theta i}(t),\ z_{\psi i}(t)]^{\mathrm{T}} = \Theta_i(t) - \Theta_{\mathrm{d}i}(t), \tag{17}$$

where $\Theta_{\mathrm{d}i}(t) = [\phi_{\mathrm{d}i}(t),\ \theta_{\mathrm{d}i}(t),\ \psi_{\mathrm{d}i}(t)]^{\mathrm{T}} \in \mathbb{R}^3$ is the desired attitude to be specified later.

E. Control Objective

The **control objective** for the path-following formation tracking problem is to design a control framework for the ith quadrotor ($i = 1, \cdots, N$) such that:

1) The LOS distance tracking error $d_{\mathrm{e}i}(t, s_i(t), d_{\mathrm{a}i}(t))$ for the ith quadrotor can converge into an arbitrarily small neighborhood of the equilibrium;

2) The LOS relative distance tracking error $d_{\mathrm{e}ij}(t, s_i(t), d_{\mathrm{a}i}(t), s_j(t), d_{\mathrm{a}j}(t))$ between the ith and jth ($j \in \mathcal{N}_i$) quadrotors can converge into an arbitrarily small neighborhood of zero;

3) For the ith quadrotor, the attitude tracking error $z_{\Theta i}(t) = [z_{\phi i}(t),\ z_{\theta i}(t),\ z_{\psi i}(t)]^{\mathrm{T}}$ can converge into an arbitrarily small neighborhood of zero;

4) The ith quadrotor satisfies its desired speed assignment $v_{\mathrm{d}i}(s_i(t), d_{\mathrm{a}i}(t))$. That is, $z_{si}(t) = \dot{s}_i(t) - v_{\mathrm{d}i}(s_i(t), d_{\mathrm{a}i}(t))$, can converge into an arbitrarily small neighborhood of zero;

5) The environment-aware dynamic constraints (13), (14), and (16) will not be violated during the formation operation.

Next, we introduce the following unit vectors before presenting the assumptions needed for analysis and discussion of our main theoretical results. First, the unit vector between the ith quadrotor and attacker is defined as $E_{\mathrm{a}i} = \frac{1}{d_{\mathrm{a}i}}[x_i - x_{\mathrm{a}},\ y_i - y_{\mathrm{a}},\ z_i - z_{\mathrm{a}}]^{\mathrm{T}} \in \mathrm{S}^2$. Similarly, the unit vector between the ith quadrotor and its desired path $E_{\mathrm{e}i}$ and unit vectors between the ith quadrotor and its neighboring agents E_{dij} ($j \in \mathcal{N}_i$) are defined as $E_{\mathrm{e}i} = \frac{1}{d_{\mathrm{e}i}}[x_i - x_{\mathrm{d}i},\ y_i - y_{\mathrm{d}i},\ z_i - z_{\mathrm{d}i}]^{\mathrm{T}} \in \mathrm{S}^2$ and $E_{dij} = \frac{1}{d_{ij}}[x_i - x_j,\ y_i - y_j,\ z_i - z_j]^{\mathrm{T}} \in \mathrm{S}^2$.

Assumption 2.1: For the ith quadrotor ($i = 1, \cdots, N$), the physical attacker is "avoidable", which requires unit vectors $E_{\mathrm{a}i}$, $E_{\mathrm{e}i}$, and E_{dij} ($j \in \mathcal{N}_i$) are not on the same plane.

Remark 2.2: For the ith quadrotor, Assumption 2.1 means that its position $p_i(t)$, desired path coordinate $p_{\mathrm{d}i}(s_i(t), d_{\mathrm{a}i}(t))$, neighboring agents position $p_j(t)$ ($j \in \mathcal{N}_i$), and the attacker position $p_{\mathrm{a}}(t)$ cannot be on the same plane. When Assumption 2.1 is satisfied, the control law u_i introduced in (33) will be non-singular. More discussion can be seen in Remark 3.3.

Remark 2.3: It is worth pointing out that Assumption 2.1 is not restrictive. Note that the desired path coordinate $p_{\mathrm{d}i}(s_i(t), d_{\mathrm{a}i}(t))$ for the ith quadrotor can depend on both the path parameter $s_i(t)$ and LOS attacker distance $d_{\mathrm{a}i}(t)$, which has two degrees of freedom. Therefore it is relatively easy to modify the desired path coordinate to satisfy this "avoidability" assumption.

Assumption 2.2: The ith UAV desired path $p_{\mathrm{d}i}(s_i(t), d_{\mathrm{a}i}(t))$ and desired path speed $v_{\mathrm{d}i}(s_i(t), d_{\mathrm{a}i}(t))$ are at least three-times and twice continuously differentiable, respectively, with bounded derivatives concerning $s_i(t)$ and $d_{\mathrm{a}i}(t)$. Furthermore, for the reference attitude we require that $\phi_{\mathrm{d}i}(t) \in (-\frac{\pi}{2},\ \frac{\pi}{2})$, $\theta_{\mathrm{d}i}(t) \in (-\frac{\pi}{2},\ \frac{\pi}{2})$, and $\psi_{\mathrm{d}i}(t) \in [-\pi,\ \pi]$, where $\psi_{\mathrm{d}i}(t)$ is at least once continuously differentiable and has bounded derivatives with respect to time.

Assumption 2.3 ([37], [38]): The thrust $F_i(t)$ and external disturbances $N_{1i}(t)$ and $N_{2i}(t)$ for the ith quadrotor are uniformly bounded with *unknown* bounds.

Assumption 2.4: The attacker velocity is continuous and is related with the relative positions between the quadrotors and attacker, that is, the attacker velocity can be expressed as $v_{\mathrm{a}}(Z_{\mathrm{a}})$ with $Z_{\mathrm{a}} = [\underbrace{\cdots,\ x_i - x_{\mathrm{a}},\ y_i - y_{\mathrm{a}},\ z_i - z_{\mathrm{a}},\ \cdots}_{i = 1, \cdots, N}]^{\mathrm{T}} \in \mathbb{R}^{3N}$. Furthermore, the attacker velocity $v_{\mathrm{a}}(Z_{\mathrm{a}})$ is *unknown*.

Remark 2.4: Assumption 2.4 means that the physical attacker has a certain level of intelligence. Therefore, the physical attacker problem considered in this work cannot be addressed by well-established obstacle-avoidance mechanisms that only consider static or time-varying obstacles.

Assumption 2.5: The mass m_i for the ith quadrotor ($i = 1, \cdots, N$) is known. However, the ith UAV inertia J_i is *unknown* such that for any $z \in \mathbb{R}^3$, $\underline{J}_i z^{\mathrm{T}} z < z^{\mathrm{T}} J_i z < \bar{J}_i z^{\mathrm{T}} z$, where $\bar{J}_i$ and $\underline{J}_i$ are *unknown* positive constants. As a direct result, the symmetric positive definite inertia matrix $M_i(\Theta_i)$ in (60) is also *unknown* and bounded, such that for any $z \in \mathbb{R}^3$, $\underline{M}_i z^{\mathrm{T}} z < z^{\mathrm{T}} M_i(\Theta_i) z < \bar{M}_i z^{\mathrm{T}} z$, where $\bar{M}_i$ and $\underline{M}_i$ are *unknown* positive constants.

Assumption 2.6 ([38]): The attitude of the ith quadrotor is confined such that $\phi_i \in (-\frac{\pi}{2},\ \frac{\pi}{2})$, $\theta_i \in (-\frac{\pi}{2} + \varepsilon_{\theta i},\ \frac{\pi}{2} - \varepsilon_{\theta i})$ and $\psi_i \in [-\pi,\ \pi]$ for some $\varepsilon_{\theta i} > 0$.

Remark 2.5: From (1)–(3), we see that quadrotors' position and attitude dynamics are highly coupled. For example, left/right movement can be archived by rolling, and forward/backward motion can be realized by pitching. Hence improper roll and pitch motions can cause aggressive motions

of quadrotors, which will not only affect system performance but can also destabilize the quadrotor dynamics and result in system failure.

The following lemmas are required for the controller design and theoretical analysis to be presented.

Lemma 2.1 ([39]): For any constant $\varepsilon > 0$ and any variable $z \in \mathbb{R}$, we have $0 \leq |z| - \frac{z^2}{\sqrt{z^2+\varepsilon^2}} < \varepsilon$.

Lemma 2.2 ([40]): Let $A \in \mathbb{R}^{n\times m}$, $B \in \mathbb{R}^{m\times l}$, and $C \in \mathbb{R}^{l\times k}$. Then $\mathrm{vec}(ABC) = (C^{\mathrm{T}} \otimes A)\mathrm{vec}(B)$.

To simplify the discussion and analysis to be presented, we will omit the variables' dependence on time, state, and path parameters when there is no potential for any confusion.

F. Radical Basis Function Neural Networks

In our formation control design, radical basis function neural networks (RBFNNs) [41]–[45] will be utilized to estimate the unknown attacker velocity $v_{\mathrm{a}}(Z_{\mathrm{a}}) : \mathbb{R}^{3N} \to \mathbb{R}^3$. Specifically, for a continuous nonlinear function $v_{\mathrm{a}}(Z_{\mathrm{a}})$ defined over a compact set $\Omega_{Z\mathrm{a}} \subset \mathbb{R}^{3N}$, there exist RBFNNs $W_{\mathrm{a}}^{\mathrm{T}} B_{\mathrm{a}}(Z_{\mathrm{a}})$ given as

$$v_{\mathrm{a}}(Z_{\mathrm{a}}) = W_{\mathrm{a}}^{\mathrm{T}} B_{\mathrm{a}}(Z_{\mathrm{a}}) + \epsilon_{\mathrm{a}}(Z_{\mathrm{a}}),$$

where $Z_{\mathrm{a}} \in \Omega_{Z\mathrm{a}} \subset \mathbb{R}^{3N}$ is the input vector, $W_{\mathrm{a}} = [w_{\mathrm{a}1}, \cdots, w_{\mathrm{a}n}]^{\mathrm{T}} \in \mathbb{R}^{n\times 3}$ is the ideal weight matrix where $w_{\mathrm{a}k} = [w_{\mathrm{a}k1},\ w_{\mathrm{a}k2},\ w_{\mathrm{a}k3}]^{\mathrm{T}} \in \mathbb{R}^3$ $(k = 1, \cdots, n)$, $n \geq 1$ is the number of neural network nodes, $B_{\mathrm{a}}(Z_{\mathrm{a}}) = [b_1(Z_{\mathrm{a}}), \cdots, b_n(Z_{\mathrm{a}})]^{\mathrm{T}} \in \mathbb{R}^n$ is the basis function vector, and $\epsilon_{\mathrm{a}}(Z_{\mathrm{a}}) = [\epsilon_{\mathrm{a}1}(Z_{\mathrm{a}}),\ \epsilon_{\mathrm{a}2}(Z_{\mathrm{a}}),\ \epsilon_{\mathrm{a}3}(Z_{\mathrm{a}})]^{\mathrm{T}} \in \mathbb{R}^3$ is the approximation error satisfying $||\epsilon_{\mathrm{a}}(Z_{\mathrm{a}})|| \leq \bar{\epsilon}_{\mathrm{a}}$, where $\bar{\epsilon}_{\mathrm{a}} > 0$ is a given precision level. The basis function $b_k(Z_{\mathrm{a}})$ is usually selected as the following Gaussian-like function [46]–[48]

$$b_k(Z_{\mathrm{a}}) = \exp\left[-\frac{(Z_{\mathrm{a}} - \nu_k)^{\mathrm{T}}(Z_{\mathrm{a}} - \nu_k)}{\zeta_k^2} \right], \quad k = 1, \cdots, n,$$

with $\nu_k = [\nu_{k1}, \cdots, \nu_{k3N}]^{\mathrm{T}} \in \mathbb{R}^{3N}$ being the receptive field's center and $\zeta_k \in \mathbb{R}$ being the width of the Gaussian-like function $b_k(Z_{\mathrm{a}})$. Moreover, W_{a} is defined as

$$W_{\mathrm{a}} := \arg \min_{\hat{W}_{\mathrm{a}} \in \mathbb{R}^{n\times 3}} \left\{ \sup_{Z_{\mathrm{a}} \in \Omega_{Z\mathrm{a}}} \left|\left| v_{\mathrm{a}}(Z_{\mathrm{a}}) - \hat{W}_{\mathrm{a}}^{\mathrm{T}} B_{\mathrm{a}}(Z_{\mathrm{a}}) \right|\right| \right\}.$$

G. Composite Barrier Function

Here we introduce the structure of "composite barrier function". Specifically, to address the environment-aware dynamic constraint requirements (11) and (14), which are on the LOS distance tracking error d_{ei} and attacker distance $d_{\mathrm{a}i}$, the following transformed error variables are introduced

$$\eta_{\mathrm{e}i} = \frac{\Omega_{d\mathrm{H}i} d_{\varepsilon ei}}{(\Omega_{d\mathrm{H}i} - d_{\varepsilon ei})(\varepsilon_{\mathrm{e}i} + d_{\varepsilon ei})}, \quad \eta_{\mathrm{a}i} = \frac{1}{d_{\mathrm{a}i} - \Omega_{\mathrm{a}i}}. \quad (18)$$

Note that $\eta_{ei} = 0$ only when $d_{\varepsilon ei} = 0$ and $\eta_{\mathrm{a}i} \to 0$ only when $d_{\mathrm{a}i} \to +\infty$. The "composite barrier function" to deal with the constraint requirements (11) and (14) is designed as

$$V_{ei} = \frac{1}{2}\eta_{ei}^2 + \frac{1}{2}\eta_{\mathrm{a}i}^2. \quad (19)$$

Remark 2.6: The function (19) is called "composite barrier function", since it takes environment-aware dynamic constraint requirements into consideration. Note that the performance and safety constraints are on different distance tracking variables. On the one hand, when the performance constraint (11) is to become violated, we get $d_{\varepsilon ei} \to \Omega_{d\mathrm{H}i}$, and hence $V_{\mathrm{e}i} \to +\infty$. On the other hand, when the safety constraint (14) is to become violated, we will have $d_{\mathrm{a}i} \to \Omega_{\mathrm{a}i}$, and hence $V_{\mathrm{e}i} \to +\infty$. Therefore, by keeping the "composite barrier function" uniformly bounded through closed-loop analysis, we can ensure that environment-aware dynamic constraint requirements (11) and (14) will be satisfied during the operation.

Next, regarding the environment-aware dynamic constraint requirement (16) on the LOS relative inter-quadrotor distance tracking error d_{eij} $(i = 1, \cdots, N,\ j \in \mathcal{N}_i)$, the following transformed error variable is introduced

$$\eta_{eij} = \frac{\Omega_{\mathrm{H}ij}\Omega_{\mathrm{L}ij} d_{eij}}{(\Omega_{\mathrm{H}ij} - d_{eij})(\Omega_{\mathrm{L}ij} + d_{eij})}. \quad (20)$$

The barrier function used to deal with the safety constraint requirement (16) is designed as

$$V_{eij} = \frac{1}{2}\eta_{eij}^2. \quad (21)$$

III. Control Design and Main Results

Here we present the controller design procedure based on backstepping, which will lead to our formation algorithm design and main theoretical results.

A. Distance Control Design and Results

Step 1:

First we consider the position kinematics of the quadrotors. Design the Lyapunov function as $V_1 = \sum_{i=1}^{N}\Big(V_{ei} + \sum_{j\in\mathcal{N}_i} V_{eij}\Big)$, and its time derivative leads to

$$\dot{V}_1 = \sum_{i=1}^{N}\Big(\eta_{ei}\dot{\eta}_{ei} + \eta_{\mathrm{a}i}\dot{\eta}_{\mathrm{a}i} + \sum_{j\in\mathcal{N}_i}\eta_{eij}\dot{\eta}_{eij}\Big). \quad (22)$$

For $\eta_{ei}\dot{\eta}_{ei} + \eta_{\mathrm{a}i}\dot{\eta}_{\mathrm{a}i}$ $(i = 1, \cdots, N)$ in (22) we get

$$\begin{aligned}\eta_{ei}\dot{\eta}_{ei} + \eta_{\mathrm{a}i}\dot{\eta}_{\mathrm{a}i} = {}& \eta_{ei}(g_{esi}\dot{s}_i + G_{epi}^{\mathrm{T}}\dot{p}_i - G_{\mathrm{e}ai}^{\mathrm{T}}\dot{p}_{\mathrm{a}}) \\ & + \eta_{\mathrm{a}i}(g_{\mathrm{a}si}\dot{s}_i + G_{\mathrm{a}pi}^{\mathrm{T}}\dot{p}_i - G_{\mathrm{a}ai}^{\mathrm{T}}\dot{p}_{\mathrm{a}}). \quad (23)\end{aligned}$$

where $g_{esi} \in \mathbb{R}$, $g_{\mathrm{a}si} \in \mathbb{R}$, $G_{epi} \in \mathbb{R}^3$, $G_{\mathrm{a}pi} \in \mathbb{R}^3$, $G_{\mathrm{e}ai} \in \mathbb{R}^3$, and $G_{\mathrm{a}ai} \in \mathbb{R}^3$ such that

$$\begin{aligned}
& g_{esi} \triangleq \frac{\partial \eta_{ei}}{\partial \Omega_{d\mathrm{H}i}}\frac{\partial \Omega_{d\mathrm{H}i}}{\partial s_i} - \frac{\partial \eta_{ei}}{\partial d_{\varepsilon ei}} E_{ei}^{\mathrm{T}}\frac{\partial p_{d i}}{\partial s_i}, \quad g_{\mathrm{a}si} \triangleq \frac{\partial \eta_{\mathrm{a}i}}{\partial \Omega_{\mathrm{a}i}}\frac{\mathrm{d}\Omega_{\mathrm{a}i}}{\mathrm{d}s_i} \\
& G_{\mathrm{e}ai} \triangleq \frac{\partial \eta_{ei}}{\partial \Omega_{d\mathrm{H}i}}\frac{\partial \Omega_{d\mathrm{H}i}}{\partial d_{\mathrm{a}i}} E_{\mathrm{a}i} - \frac{\partial \eta_{ei}}{\partial d_{\varepsilon ei}} E_{ei}^{\mathrm{T}}\frac{\partial p_{d i}}{\partial d_{\mathrm{a}i}} E_{\mathrm{a}i}, \\
& G_{\mathrm{a}ai} \triangleq \frac{\partial \eta_{\mathrm{a}i}}{\partial d_{\mathrm{a}i}} E_{\mathrm{a}i}, \quad G_{epi} \triangleq G_{\mathrm{e}ai} + \frac{\partial \eta_{ei}}{\partial d_{\varepsilon ei}} E_{ei}, \quad G_{\mathrm{a}pi} \triangleq G_{\mathrm{a}ai},
\end{aligned}$$

and recall $E_{\mathrm{e}i} \in \mathrm{S}^2$ and $E_{\mathrm{a}i} \in \mathrm{S}^2$ are defined in Section II-E. Similarly, for $\eta_{eij}\dot{\eta}_{eij}$ $(i = 1, \cdots, N,\ j \in \mathcal{N}_i)$ in (22) we obtain

$$\begin{aligned}\eta_{eij}\dot{\eta}_{eij} = {}& \eta_{eij}\big(g_{eijsi}\dot{s}_i + g_{eijsj}\dot{s}_j + G_{eijpi}^{\mathrm{T}}\dot{p}_i + G_{eijpj}^{\mathrm{T}}\dot{p}_j \\ & - G_{aij}^{\mathrm{T}}\dot{p}_{\mathrm{a}}\big), \quad (24)\end{aligned}$$

where

$$\begin{aligned}
g_{eijsi} &\triangleq \frac{\partial \eta_{eij}}{\partial \Omega_{\mathrm{H}ij}}\frac{\partial \Omega_{\mathrm{H}ij}}{\partial s_i} + \frac{\partial \eta_{eij}}{\partial \Omega_{\mathrm{L}ij}}\frac{\partial \Omega_{\mathrm{L}ij}}{\partial s_i} \\
&\quad - \frac{\partial \eta_{eij}}{\partial d_{eij}} E_{Lij}^{\mathrm{T}} \frac{\partial p_{\mathrm{d}i}}{\partial s_i}, \quad g_{eijsi} \in \mathbb{R}, \\
g_{eijsj} &\triangleq \frac{\partial \eta_{eij}}{\partial \Omega_{\mathrm{H}ij}}\frac{\partial \Omega_{\mathrm{H}ij}}{\partial s_j} + \frac{\partial \eta_{eij}}{\partial \Omega_{\mathrm{L}ij}}\frac{\partial \Omega_{\mathrm{L}ij}}{\partial s_j} \\
&\quad + \frac{\partial \eta_{eij}}{\partial d_{eij}} E_{Lij}^{\mathrm{T}} \frac{\partial p_{\mathrm{d}j}}{\partial s_j}, \quad g_{\eta ijsj} \in \mathbb{R}, \\
G_{eijpi} &\triangleq \frac{\partial \eta_{eij}}{\partial \Omega_{\mathrm{H}ij}}\frac{\partial \Omega_{\mathrm{H}ij}}{\partial d_{\mathrm{a}i}} E_{\mathrm{a}i} + \frac{\partial \eta_{eij}}{\partial \Omega_{\mathrm{L}ij}}\frac{\partial \Omega_{\mathrm{L}ij}}{\partial d_{\mathrm{a}i}} E_{\mathrm{a}i} \\
&\quad + \frac{\partial \eta_{eij}}{\partial d_{eij}} E_{dij} - \frac{\partial \eta_{eij}}{\partial d_{eij}} E_{Lij}^{\mathrm{T}} \frac{\partial p_{\mathrm{d}i}}{\partial d_{\mathrm{a}i}} E_{\mathrm{a}i}, \\
G_{eijpj} &\triangleq \frac{\partial \eta_{eij}}{\partial \Omega_{\mathrm{H}ij}}\frac{\partial \Omega_{\mathrm{H}ij}}{\partial d_{\mathrm{a}j}} E_{\mathrm{a}j} + \frac{\partial \eta_{eij}}{\partial \Omega_{\mathrm{L}ij}}\frac{\partial \Omega_{\mathrm{L}ij}}{\partial d_{\mathrm{a}j}} E_{\mathrm{a}j} \\
&\quad - \frac{\partial \eta_{eij}}{\partial d_{eij}} E_{dij} + \frac{\partial \eta_{eij}}{\partial d_{eij}} E_{Lij}^{\mathrm{T}} \frac{\partial p_{\mathrm{d}j}}{\partial d_{\mathrm{a}j}} E_{\mathrm{a}j}, \\
G_{\mathrm{a}ij} &\triangleq G_{eijpi} + G_{eijpj}, \quad G_{eijpi}, G_{eijpj}, G_{\mathrm{a}ij} \in \mathbb{R}^3,
\end{aligned}$$

in which recall $E_{dij} \in \mathrm{S}^2$ is defined in Assumption 2.1. Furthermore, unit vectors $E_{Lij} \in \mathrm{S}^2$ and $E_{\mathrm{a}j} \in \mathrm{S}^2$ are defined as $E_{Lij} = \frac{1}{L_{ij}}[x_{\mathrm{d}i} - x_{\mathrm{d}j},\ y_{\mathrm{d}i} - y_{\mathrm{d}j},\ z_{\mathrm{d}i} - z_{\mathrm{d}j}]^{\mathrm{T}}$ and $E_{\mathrm{a}j} = \frac{1}{d_{\mathrm{a}j}}[x_j - x_{\mathrm{a}},\ y_j - y_{\mathrm{a}},\ z_j - z_{\mathrm{a}}]^{\mathrm{T}}$, respectively.

Hence, from (22), $\dot{V}_1$ yields to

$$\dot{V}_1 = \sum_{i=1}^{N}\Big(h_{si}\dot{s}_i + H_{pi}^{\mathrm{T}}\dot{p}_i - H_{\mathrm{a}i}^{\mathrm{T}}\dot{p}_{\mathrm{a}}\Big), \tag{25}$$

where

$$\begin{aligned}
h_{si} &= \eta_{\mathrm{e}i}g_{esi} + \eta_{\mathrm{a}i}g_{\mathrm{a}si} + 2\sum_{j\in\mathcal{N}_i}\eta_{eij}g_{eijsi}, \quad h_{si} \in \mathbb{R}, \\
H_{pi} &= \eta_{\mathrm{e}i}G_{epi} + \eta_{\mathrm{a}i}G_{\mathrm{a}pi} + 2\sum_{j\in\mathcal{N}_i}\eta_{eij}G_{eijpi}, \quad H_{pi} \in \mathbb{R}^3, \\
H_{\mathrm{a}i} &= \eta_{\mathrm{e}i}G_{\mathrm{e}ai} + \eta_{\mathrm{a}i}G_{\mathrm{a}ai} + 2\sum_{j\in\mathcal{N}_i}\eta_{eij}G_{eijpi}, \quad H_{\mathrm{a}i} \in \mathbb{R}^3.
\end{aligned}$$

Moreover, the term H_{pi} in (25) can be rewritten as

$$H_{pi} = h_{\mathrm{pa}i}E_{\mathrm{a}i} + h_{\mathrm{pe}i}E_{\mathrm{e}i} + \sum_{j\in\mathcal{N}_i}h_{pdij}E_{dij} = E_{pi}^{\mathrm{T}}h_{pi}, \tag{26}$$

where

$$\begin{aligned}
h_{\mathrm{pa}i} &= \eta_{\mathrm{e}i}\left(\frac{\partial \eta_{\mathrm{e}i}}{\partial \Omega_{d\mathrm{H}i}}\frac{\partial \Omega_{d\mathrm{H}i}}{\partial d_{\mathrm{a}i}} - \frac{\partial \eta_{\mathrm{e}i}}{\partial d_{\varepsilon ei}}E_{\mathrm{e}i}^{\mathrm{T}}\frac{\partial p_{\mathrm{d}i}}{\partial d_{\mathrm{a}i}}\right) + \eta_{\mathrm{a}i}\frac{\partial \eta_{\mathrm{a}i}}{\partial d_{\mathrm{a}i}} \\
&\quad + 2\sum_{j\in\mathcal{N}_i}\eta_{eij}\left(\frac{\partial \eta_{eij}}{\partial \Omega_{\mathrm{H}ij}}\frac{\partial \Omega_{\mathrm{H}ij}}{\partial d_{\mathrm{a}i}} + \frac{\partial \eta_{eij}}{\partial \Omega_{\mathrm{L}ij}}\frac{\partial \Omega_{\mathrm{L}ij}}{\partial d_{\mathrm{a}i}}\right. \\
&\quad \left. - \frac{\partial \eta_{eij}}{\partial d_{eij}}E_{Lij}^{\mathrm{T}}\frac{\partial p_{\mathrm{d}i}}{\partial d_{\mathrm{a}i}}\right) \in \mathbb{R}, \\
h_{\mathrm{pe}i} &= \eta_{\mathrm{e}i}\frac{\partial \eta_{\mathrm{e}i}}{\partial d_{\varepsilon ei}} \in \mathbb{R}, \quad h_{pdij} = 2\eta_{eij}\frac{\partial \eta_{eij}}{\partial d_{eij}} \in \mathbb{R}, \\
h_{pi} &= [h_{\mathrm{pa}i},\ h_{\mathrm{pe}i},\ \underbrace{\cdots,\ h_{pdij},\ \cdots}_{j\in\mathcal{N}_i}]^{\mathrm{T}} \in \mathbb{R}^{|\mathcal{N}_i|+2}, \\
E_{pi} &= [E_{\mathrm{a}i},\ E_{\mathrm{e}i},\ \underbrace{\cdots,\ E_{dij},\ \cdots}_{j\in\mathcal{N}_i}]^{\mathrm{T}} \in \mathbb{R}^{(|\mathcal{N}_i|+2)\times 3}.
\end{aligned}$$

Now, taking (26) into (25) yields

$$\dot{V}_1 = \sum_{i=1}^{N}\Big(h_{si}\dot{s}_i + h_{pi}^{\mathrm{T}}E_{pi}\dot{p}_i - H_{\mathrm{a}i}^{\mathrm{T}}\dot{p}_{\mathrm{a}}\Big), \tag{27}$$

where, by using Lemmas 2.1 and 2.2, the term $-H_{\mathrm{a}i}^{\mathrm{T}}\dot{p}_{\mathrm{a}}$ $(i = 1, \cdots, N)$ can be expressed as follows

$$\begin{aligned}
-H_{\mathrm{a}i}^{\mathrm{T}}\dot{p}_{\mathrm{a}} &= -H_{\mathrm{a}i}^{\mathrm{T}}\Big(W_{\mathrm{a}}^{\mathrm{T}}(B_{\mathrm{a}}(Z_{\mathrm{a}}) - B_{\mathrm{a}i} + B_{\mathrm{a}i}) + \epsilon_{\mathrm{a}}(Z_{\mathrm{a}})\Big) \\
&\le -H_{\mathrm{a}i}^{\mathrm{T}}(\hat{W}_{\mathrm{a}i}^{\mathrm{T}} - \tilde{W}_{\mathrm{a}i}^{\mathrm{T}})B_{\mathrm{a}i} + \bar{\delta}_{\mathrm{a}}\,||H_{\mathrm{a}i}|| \\
&< -\hat{w}_{\mathrm{a}i}^{\mathrm{T}}(H_{\mathrm{a}i}\otimes B_{\mathrm{a}i}) + \tilde{w}_{\mathrm{a}i}^{\mathrm{T}}(H_{\mathrm{a}i}\otimes B_{\mathrm{a}i}) \\
&\quad + \bar{\delta}_{\mathrm{a}}\frac{||H_{\mathrm{a}i}||^2}{\sqrt{||H_{\mathrm{a}i}||^2 + \varepsilon_i^2}} + \bar{\delta}_{\mathrm{a}}\varepsilon_i,
\end{aligned}$$

where $\tilde{W}_{\mathrm{a}i} = \hat{W}_{\mathrm{a}i} - W_{\mathrm{a}}$, $\hat{W}_{\mathrm{a}i} \in \mathbb{R}^{n\times 3}$ is the estimation of W_{a} by the ith quadrotor, $\hat{w}_{\mathrm{a}i} = \mathrm{vec}(\hat{W}_{\mathrm{a}i}^{\mathrm{T}}) \in \mathbb{R}^{3n}$, $w_{\mathrm{a}} = \mathrm{vec}(W_{\mathrm{a}}^{\mathrm{T}}) \in \mathbb{R}^{3n}$, $\tilde{w}_{\mathrm{a}i} = \mathrm{vec}(\tilde{W}_{\mathrm{a}i}^{\mathrm{T}}) \in \mathbb{R}^{3n}$, $\bar{\delta}_{\mathrm{a}} \triangleq \sqrt{n}\,||W_{\mathrm{a}}|| + \bar{\epsilon}_{\mathrm{a}}$ is unknown, and $B_{\mathrm{a}i} \triangleq B_{\mathrm{a}}(Z_{\mathrm{a}i})$ with $Z_{\mathrm{a}i} = [x_i - x_{\mathrm{a}},\ y_i - y_{\mathrm{a}},\ z_i - z_{\mathrm{a}},\ \underbrace{\cdots,\ x_j - x_{\mathrm{a}},\ y_j - y_{\mathrm{a}},\ z_j - z_{\mathrm{a}},\ \cdots}_{j\in\mathcal{N}_i}]^{\mathrm{T}} \in \mathbb{R}^{3|\mathcal{N}_i|+3}$. Besides, $\varepsilon_i > 0$ is an arbitrarily small number introduced in view of Lemma 2.1.

Next, define the fictitious velocity tracking error as $z_{vi} = E_{pi}\dot{p}_i - \alpha_{pi}$, with the stabilizing function $\alpha_{pi} \in \mathbb{R}^{|\mathcal{N}_i|+2}$ $(i = 1, \cdots, N)$ designed as

$$\begin{aligned}
\alpha_{pi} = \frac{h_{pi}}{h_{pi}^{\mathrm{T}}h_{pi}}\Bigg(&-K_{\mathrm{e}i}\eta_{\mathrm{e}i}^2 - K_{\mathrm{a}i}\eta_{\mathrm{a}i}^2 - \sum_{j\in\mathcal{N}_i}K_{eij}\eta_{eij}^2 - h_{si}v_{\mathrm{d}i} \\
&+ \hat{w}_{\mathrm{a}i}^{\mathrm{T}}(H_{\mathrm{a}i}\otimes B_{\mathrm{a}i}) - \hat{\bar{\delta}}_{\mathrm{a}i}\frac{||H_{\mathrm{a}i}||^2}{\sqrt{||H_{\mathrm{a}i}||^2 + \varepsilon_i^2}}\Bigg),
\end{aligned} \tag{28}$$

where $K_{\mathrm{e}i} > 0$, $K_{\mathrm{a}i} > 0$, and $K_{eij} > 0$ are the control gains and $\hat{\bar{\delta}}_{\mathrm{a}i}$ is the estimation of $\bar{\delta}_{\mathrm{a}}$.

Remark 3.1: In (28), $||h_{pi}|| = 0$ does not cause singularity in the stabilizing function design. $||h_{pi}|| = 0$ implies that $h_{\mathrm{pa}i} = 0$, $h_{\mathrm{pe}i} = 0$, and $h_{pdij} = 0$ $(j \in \mathcal{N}_i)$ at the same time, which implies $\eta_{\mathrm{e}i} = 0$, $\eta_{\mathrm{a}i} = 0$, and $\eta_{eij} = 0$. When this happens, all terms inside the bracket on the right-hand-side of (28) are zero. According to L'Hôpital's rule, we have $\lim_{||h_{pi}||\to 0}\alpha_{pi} = \alpha_{pi}(v_{\mathrm{d}i}, \hat{w}_{\mathrm{a}i}, \hat{\bar{\delta}}_{\mathrm{a}i})$. Since $v_{\mathrm{d}i}$ is the desired speed assignment along the path, which is selected as a bounded function, and the boundedness of $\hat{w}_{\mathrm{a}i}$ and $\hat{\bar{\delta}}_{\mathrm{a}i}$ is to be shown in Theorem 3.1, hence $\alpha_{pi}(v_{\mathrm{d}i}, \hat{w}_{\mathrm{a}i}, \hat{\bar{\delta}}_{\mathrm{a}i})$ is bounded. Thus, singularity of α_{pi} will not happen.

Hence, (27) yields

$$\begin{aligned}
\dot{V}_1 < \sum_{i=1}^{N}\Bigg(&h_{pi}^{\mathrm{T}}z_{vi} - K_{\mathrm{e}i}\eta_{\mathrm{e}i}^2 - K_{\mathrm{a}i}\eta_{\mathrm{a}i}^2 - \sum_{j\in\mathcal{N}_i}K_{eij}\eta_{eij}^2 \\
&+ h_{si}z_{si} + \tilde{w}_{\mathrm{a}i}^{\mathrm{T}}(H_{\mathrm{a}i}\otimes B_{\mathrm{a}i}) \\
&- \tilde{\bar{\delta}}_{\mathrm{a}i}\frac{||H_{\mathrm{a}i}||^2}{\sqrt{||H_{\mathrm{a}i}||^2 + \varepsilon_i^2}} + \bar{\delta}_{\mathrm{a}}\varepsilon_i\Bigg),
\end{aligned} \tag{29}$$

where $\tilde{\bar{\delta}}_{\mathrm{a}i} = \hat{\bar{\delta}}_{\mathrm{a}i} - \bar{\delta}_{\mathrm{a}}$ and the path speed error is defined as $z_{si} = \dot{s}_i - v_{\mathrm{d}i}$.

Step 2:

At this step, we consider the translational dynamics of the quadrotors. Design the Lyapunov function candidate at this step as $V_2 = \sum_{i=1}^{N} \frac{1}{2} z_{vi}^{\mathrm{T}} z_{vi}$, and its time derivative gives

$$\dot{V}_2 = \sum_{i=1}^{N} z_{vi}^{\mathrm{T}} \Big[E_{pi} g e_z - \frac{1}{m_i} u_{i0} - \frac{1}{m_i} E_{pi} F_i (R_i - R_{\mathrm{d}i}) e_z + \frac{1}{m_i} E_{pi} N_{1i} + \dot{E}_{pi} \dot{p}_i - \dot{\alpha}_{pi} \Big], \tag{30}$$

in which we denote $u_{i0} = E_{pi} u_i \in \mathbb{R}^{|\mathcal{N}_i|+2}$, $u_i = F_i R_{\mathrm{d}i} e_z \in \mathbb{R}^3$, and

$$\begin{aligned} \dot{\alpha}_{pi} &= H_{\alpha \mathrm{a}i} (\dot{p}_i - \dot{p}_{\mathrm{a}}) + \sum_{j \in \mathcal{N}_i} H_{\alpha \mathrm{a}ij} (\dot{p}_j - \dot{p}_{\mathrm{a}}) + H_{\alpha pi} \dot{p}_i \\ &\quad + \sum_{j \in \mathcal{N}_i} H_{\alpha pij} (\dot{p}_i - \dot{p}_j) + h_{\alpha si} \dot{s}_i + \sum_{j \in \mathcal{N}_i} h_{\alpha sij} \dot{s}_j \\ &\quad + \frac{\partial \alpha_{pi}}{\partial \hat{w}_{\mathrm{a}i}} \dot{\hat{w}}_{\mathrm{a}i} + \frac{\partial \alpha_{pi}}{\partial \hat{\delta}_{\mathrm{a}i}} \dot{\hat{\delta}}_{\mathrm{a}i} \\ &= H_{\alpha pi} \dot{p}_i + G_{\alpha \mathrm{a}i} (\dot{p}_i - \dot{p}_{\mathrm{a}}) + \sum_{j \in \mathcal{N}_i} G_{\alpha pij} (\dot{p}_i - \dot{p}_j) \\ &\quad + h_{\alpha si} \dot{s}_i + \sum_{j \in \mathcal{N}_i} h_{\alpha sij} \dot{s}_j + \frac{\partial \alpha_{pi}}{\partial \hat{w}_{\mathrm{a}i}} \dot{\hat{w}}_{\mathrm{a}i} + \frac{\partial \alpha_{pi}}{\partial \hat{\delta}_{\mathrm{a}i}} \dot{\hat{\delta}}_{\mathrm{a}i}, \end{aligned} \tag{31}$$

where $G_{\alpha \mathrm{a}i} = H_{\alpha \mathrm{a}i} + \sum_{j \in \mathcal{N}_i} H_{\alpha \mathrm{a}ij}$ and $G_{\alpha pij} = H_{\alpha pij} - H_{\alpha \mathrm{a}ij}$, with $H_{\alpha pi} = \frac{\partial \alpha_{pi}}{\partial (p_i - p_{\mathrm{d}i})} \in \mathbb{R}^{(|\mathcal{N}_i|+2)\times 3}$ and $H_{\alpha pij} = \frac{\partial \alpha_{pi}}{\partial (p_i - p_j)} \in \mathbb{R}^{(|\mathcal{N}_i|+2)\times 3}$. Moreover, $H_{\alpha \mathrm{a}i} \in \mathbb{R}^{(|\mathcal{N}_i|+2)\times 3}$, $H_{\alpha \mathrm{a}ij} \in \mathbb{R}^{(|\mathcal{N}_i|+2)\times 3}$, $h_{\alpha si} \in \mathbb{R}^{|\mathcal{N}_i|+2}$ and $h_{\alpha sij} \in \mathbb{R}^{|\mathcal{N}_i|+2}$ are given in Appendix B (see (62)–(65)). Moreover, $\dot{E}_{pi} \dot{p}_i$ in (30) can be expressed as

$$\dot{E}_{pi} \dot{p}_i = \xi_{pi} \dot{p}_i + \xi_{\mathrm{a}i} \dot{p}_{\mathrm{a}} + \xi_{si} \dot{s}_i + \sum_{j \in \mathcal{N}_i} E_{pdij} (\dot{p}_i - \dot{p}_j), \tag{32}$$

where

$$\begin{aligned} \xi_{pi} &= E_{\mathrm{pa}i} + E_{\mathrm{pe}i} - E_{\mathrm{pe}i} \frac{\partial p_{\mathrm{d}i}}{\partial d_{\mathrm{a}i}} E_{\mathrm{a}i}^{\mathrm{T}}, \quad \xi_{pi} \in \mathbb{R}^{(|\mathcal{N}_i|+2)\times 3}, \\ \xi_{\mathrm{a}i} &= -E_{\mathrm{pa}i} + E_{\mathrm{pe}i} \frac{\partial p_{\mathrm{d}i}}{\partial d_{\mathrm{a}i}} E_{\mathrm{a}i}^{\mathrm{T}}, \quad \xi_{\mathrm{a}i} \in \mathbb{R}^{(|\mathcal{N}_i|+2)\times 3}, \\ \xi_{si} &= -E_{\mathrm{pe}i} \frac{\partial p_{\mathrm{d}i}}{\partial s_i}, \quad \xi_{si} \in \mathbb{R}^{|\mathcal{N}_i|+2}, \end{aligned}$$

in which $E_{\mathrm{pa}i}$, $E_{\mathrm{pe}i}$, and E_{pdij} are expressed as

$$\begin{aligned} E_{\mathrm{pa}i} &= [Q_{\mathrm{a}i}^{\mathrm{T}} \dot{p}_i, \quad \underbrace{0_3, \ \cdots, \ 0_3}_{|\mathcal{N}_i| + 1 \text{ zero vectors}} \ ]^{\mathrm{T}} \in \mathbb{R}^{(|\mathcal{N}_i|+2)\times 3}, \\ E_{\mathrm{pe}i} &= [0_3, \ Q_{\mathrm{e}i}^{\mathrm{T}} \dot{p}_i, \ \underbrace{0_3, \ \cdots, \ 0_3}_{|\mathcal{N}_i| \text{ zero vectors}}]^{\mathrm{T}} \in \mathbb{R}^{(|\mathcal{N}_i|+2)\times 3}, \\ E_{pdij} &= [0_3, \ 0_3, \ \cdots, \ Q_{dij}^{\mathrm{T}} \dot{p}_i, \ \cdots]^{\mathrm{T}} \in \mathbb{R}^{(|\mathcal{N}_i|+2)\times 3}, \end{aligned}$$

where $0_3 = [0, \ 0, \ 0]^{\mathrm{T}} \in \mathbb{R}^3$, $Q_{\mathrm{a}i} = \frac{d_{\mathrm{a}i} I_3 - (p_i - p_{\mathrm{a}}) E_{\mathrm{a}i}^{\mathrm{T}}}{d_{\mathrm{a}i}^2} \in \mathbb{R}^{3\times 3}$, $Q_{\mathrm{e}i} = \frac{d_{\mathrm{e}i} I_3 - (p_i - p_{\mathrm{d}i}) E_{\mathrm{e}i}^{\mathrm{T}}}{d_{\mathrm{e}i}^2} \in \mathbb{R}^{3\times 3}$, and $Q_{dij} = \frac{d_{ij} I_3 - (p_i - p_j) E_{dij}^{\mathrm{T}}}{d_{ij}^2} \in \mathbb{R}^{3\times 3}$, $j \in \mathcal{N}_i$. For the matrix E_{pdij}, $j \in \mathcal{N}_i$, the $(2 + I_{ij})$th column vector is $Q_{dij}^{\mathrm{T}} \dot{p}_i$ and other columns are zero vectors, where I_{ij} is the index of j in the set $\mathcal{N}_i$.

Remark 3.2: In (32), singularity can only happen when $d_{\mathrm{e}i} = 0$, $d_{\mathrm{a}i} = 0$, or $d_{ij} = 0$, $j \in \mathcal{N}_i$. However, in view of the performance and safety constraint requirements (12), (14), and (16), we have $d_{\mathrm{e}i} > \varepsilon_{\mathrm{e}i} > 0$, $d_{\mathrm{a}i} > \Omega_{\mathrm{a}i} > 0$, and $d_{ij} > 0$, hence $d_{\mathrm{e}i} = 0$, $d_{\mathrm{a}i} = 0$, and $d_{ij} = 0$ will not happen if (12), (14), and (16) are satisfied. Therefore, singularity will not occur in (32).

Now, for the ith quadrotor ($i = 1, \cdots, N$), the control law $u_i \in \mathbb{R}^3$ is designed as

$$u_i = (E_{pi}^{\mathrm{T}} E_{pi})^{-1} E_{pi}^{\mathrm{T}} u_{i0}, \tag{33}$$

$$\begin{aligned} u_{i0} = m_i \Bigg[& (\xi_{pi} - H_{\alpha pi} - G_{\alpha \mathrm{a}i}) \dot{p}_i + (\xi_{si} - h_{\alpha si}) v_{\mathrm{d}i} \\ & - \sum_{j \in \mathcal{N}_i} h_{\alpha sij} v_{\mathrm{d}j} + \sum_{j \in \mathcal{N}_i} (E_{pdij} - G_{\alpha pij}) (\dot{p}_i - \dot{p}_j) \\ & + \hat{\delta}_{\mathrm{a}i} \frac{\xi_{\mathrm{a}i} \xi_{\mathrm{a}i}^{\mathrm{T}} z_{vi}}{\sqrt{\left|\left|\xi_{\mathrm{a}i}^{\mathrm{T}} z_{vi}\right|\right|^2 + \varepsilon_i^2}} + \hat{\delta}_i \frac{E_{pi} E_{pi}^{\mathrm{T}} z_{vi}}{\sqrt{\left|\left|E_{pi}^{\mathrm{T}} z_{vi}\right|\right|^2 + \varepsilon_i^2}} \\ & + \hat{\delta}_{\mathrm{a}i} \frac{G_{\alpha \mathrm{a}i} G_{\alpha \mathrm{a}i}^{\mathrm{T}} z_{vi}}{\sqrt{\left|\left|G_{\alpha \mathrm{a}i}^{\mathrm{T}} z_{vi}\right|\right|^2 + \varepsilon_i^2}} + \left(B_{\mathrm{a}i}^{\mathrm{T}} \otimes \xi_{\mathrm{a}i}\right) \hat{w}_{\mathrm{a}i} \\ & + \left(B_{\mathrm{a}i}^{\mathrm{T}} \otimes G_{\alpha \mathrm{a}i}\right) \hat{w}_{\mathrm{a}i} + K_{vi} z_{vi} + E_{pi} g e_z + h_{pi} \\ & - \frac{\partial \alpha_{pi}}{\partial \hat{w}_{\mathrm{a}i}} \dot{\hat{w}}_{\mathrm{a}i} - \frac{\partial \alpha_{pi}}{\partial \hat{\delta}_{\mathrm{a}i}} \dot{\hat{\delta}}_{\mathrm{a}i} \Bigg], \end{aligned} \tag{34}$$

where $K_{vi} > 0$ is a control gain, $\varepsilon_i > 0$ is a design constant, and $\hat{\delta}_i$ is the estimation of the unknown constant $\bar{\delta}_i$ satisfying $\left|\left| -\frac{1}{m_i} F_i (R_i - R_{\mathrm{d}i}) e_z + \frac{1}{m_i} N_{1i} \right|\right| \leq \bar{\delta}_i$. Moreover, adaptive laws $\dot{\hat{w}}_{\mathrm{a}i}$ and $\dot{\hat{\delta}}_{\mathrm{a}i}$ will be introduced in (39) and (40), respectively.

Remark 3.3: In (33), the square matrix $E_{pi}^{\mathrm{T}} E_{pi} \in \mathbb{R}^{3\times 3}$ is required to be invertible to ensure that the control law u_i is non-singular. According to the definition of $E_{pi} \in \mathbb{R}^{(|\mathcal{N}_i|+2)\times 3}$ in (26), $\mathrm{rank}(E_{pi}) = \mathrm{rank}(E_{pi}^{\mathrm{T}}) = \min(|\mathcal{N}_i|+2, \ 3) = 3$ since each agent in the group has at least one neighbor ($|\mathcal{N}_i| \geq 1$) and the "avoidable" condition in Assumption 2.1 is satisfied during the operation. Therefore, $\mathrm{rank}(E_{pi}^{\mathrm{T}} E_{pi}) = 3$, hence $E_{pi}^{\mathrm{T}} E_{pi}$ is invertible.

Remark 3.4: In (34), we can observe that the relative velocities between each UAV and its neighboring agents are used for the controller design. This condition is not restrictive in practical applications since it can be easily achieved by methods such as optical flow [49], [50] and visual odometry [51], [52], which does not require real-time bidirectional communications with neighboring agents.

According to (29) and (30), we can derive

$$\begin{aligned} & \dot{V}_1 + \dot{V}_2 \\ & < \sum_{i=1}^{N} \Bigg\{ - K_{\mathrm{e}i} \eta_{\mathrm{e}i}^2 - K_{\mathrm{a}i} \eta_{\mathrm{a}i}^2 - \sum_{j \in \mathcal{N}_i} K_{\mathrm{e}ij} \eta_{\mathrm{e}ij}^2 - K_{vi} z_{vi}^{\mathrm{T}} z_{vi} \\ & \quad + h_{si} z_{si} + z_{vi}^{\mathrm{T}} (\xi_{si} - h_{\alpha si}) z_{si} - \sum_{j \in \mathcal{N}_i} z_{vi}^{\mathrm{T}} h_{\alpha sij} z_{sj} \\ & \quad - \tilde{\delta}_{\mathrm{a}i} \frac{||H_{\mathrm{a}i}||^2}{\sqrt{||H_{\mathrm{a}i}||^2 + \varepsilon_i^2}} - \tilde{\delta}_{\mathrm{a}i} \frac{\left|\left|\xi_{\mathrm{a}i}^{\mathrm{T}} z_{vi}\right|\right|^2}{\sqrt{\left|\left|\xi_{\mathrm{a}i}^{\mathrm{T}} z_{vi}\right|\right|^2 + \varepsilon_i^2}} \end{aligned}$$

$$- \tilde{\delta}_{\mathrm{a}i}\frac{\left|\left|G_{\alpha \mathrm{a}i}^{\mathrm{T}} z_{vi}\right|\right|^2}{\sqrt{\left|\left|G_{\alpha \mathrm{a}i}^{\mathrm{T}} z_{vi}\right|\right|^2+\varepsilon_i^2}} - \tilde{\delta}_i\frac{\left|\left|E_{pi}^{\mathrm{T}} z_{vi}\right|\right|^2}{\sqrt{\left|\left|E_{pi}^{\mathrm{T}} z_{vi}\right|\right|^2+\varepsilon_i^2}} + \tilde{w}_{\mathrm{a}i}^{\mathrm{T}}(H_{\mathrm{a}i}\otimes B_{\mathrm{a}i}) - \tilde{w}_{\mathrm{a}i}^{\mathrm{T}}\left[(G_{\alpha \mathrm{a}i}^{\mathrm{T}} z_{vi})\otimes B_{\mathrm{a}i}\right] - \tilde{w}_{\mathrm{a}i}^{\mathrm{T}}\left[(\xi_{\mathrm{a}i}^{\mathrm{T}} z_{vi})\otimes B_{\mathrm{a}i}\right] + (3\bar{\delta}_{\mathrm{a}}+\bar{\delta}_i)\varepsilon_i\Bigg\}, \tag{35}$$

where $\tilde{\delta}_i = \hat{\delta}_i - \bar{\delta}_i$ $(i = 1, \cdots, N)$.

Next define $V_s = \sum_{i=1}^{N} \frac{1}{2} z_{si}^2$, its time derivative gives

$$\dot{V}_s = \sum_{i=1}^{N} z_{si}\left(\ddot{s}_i - \frac{\partial v_{\mathrm{d}i}}{\partial s_i}\dot{s}_i - \frac{\partial v_{\mathrm{d}i}}{\partial d_{\mathrm{a}i}} E_{\mathrm{a}i}^{\mathrm{T}}(\dot{p}_i - \dot{p}_{\mathrm{a}})\right). \tag{36}$$

Now, design the path parameter timing law $\ddot{s}_i$ $(i = 1, \cdots, N)$ as

$$\ddot{s}_i = -K_{si} z_{si} + \frac{\partial v_{\mathrm{d}i}}{\partial s_i}\dot{s}_i + \frac{\partial v_{\mathrm{d}i}}{\partial d_{\mathrm{a}i}} E_{\mathrm{a}i}^{\mathrm{T}}\dot{p}_i - z_{vi}^{\mathrm{T}}(\xi_{si} - h_{\alpha si}) + \sum_{j\in\mathcal{N}_i} z_{vj}^{\mathrm{T}} h_{\alpha sji} - \hat{\delta}_{\mathrm{a}i}\frac{z_{si}\left|\left|\frac{\partial v_{\mathrm{d}i}}{\partial d_{\mathrm{a}i}} E_{\mathrm{a}i}\right|\right|^2}{\sqrt{z_{si}^2\left|\left|\frac{\partial v_{\mathrm{d}i}}{\partial d_{\mathrm{a}i}} E_{\mathrm{a}i}\right|\right|^2+\varepsilon_i^2}} - \frac{\partial v_{\mathrm{d}i}}{\partial d_{\mathrm{a}i}}\left(E_{\mathrm{a}i}\otimes B_{\mathrm{a}i}\right)^{\mathrm{T}}\hat{w}_{\mathrm{a}i} - h_{si}, \tag{37}$$

where $s_i(0) = s_{i10}$ and $\dot{s}_i(0) = s_{i20}$ are initial conditions and $K_{si} > 0$ is a control constant.

Therefore, considering (35) and (36), we can get

$$\begin{aligned}
&\dot{V}_1 + \dot{V}_2 + \dot{V}_s \\
&< \sum_{i=1}^{N}\Bigg\{-K_{\mathrm{e}i}\eta_{\mathrm{e}i}^2 - K_{\mathrm{a}i}\eta_{\mathrm{a}i}^2 - \sum_{j\in\mathcal{N}_i} K_{\mathrm{e}ij}\eta_{\mathrm{e}ij}^2 - K_{vi} z_{vi}^{\mathrm{T}} z_{vi} \\
&\quad - K_{si} z_{si}^2 - \tilde{\delta}_{\mathrm{a}i}\frac{||H_{\mathrm{a}i}||^2}{\sqrt{||H_{\mathrm{a}i}||^2+\varepsilon_i^2}} - \tilde{\delta}_{\mathrm{a}i}\frac{\left|\left|\xi_{\mathrm{a}i}^{\mathrm{T}} z_{vi}\right|\right|^2}{\sqrt{\left|\left|\xi_{\mathrm{a}i}^{\mathrm{T}} z_{vi}\right|\right|^2+\varepsilon_i^2}} \\
&\quad - \tilde{\delta}_{\mathrm{a}i}\frac{\left|\left|G_{\alpha \mathrm{a}i}^{\mathrm{T}} z_{vi}\right|\right|^2}{\sqrt{\left|\left|G_{\alpha \mathrm{a}i}^{\mathrm{T}} z_{vi}\right|\right|^2+\varepsilon_i^2}} - \tilde{\delta}_{\mathrm{a}i}\frac{z_{si}^2\left|\left|\frac{\partial v_{\mathrm{d}i}}{\partial d_{\mathrm{a}i}} E_{\mathrm{a}i}\right|\right|^2}{\sqrt{z_{si}^2\left|\left|\frac{\partial v_{\mathrm{d}i}}{\partial d_{\mathrm{a}i}} E_{\mathrm{a}i}\right|\right|^2+\varepsilon_i^2}} \\
&\quad - \tilde{\delta}_i\frac{\left|\left|E_{pi}^{\mathrm{T}} z_{vi}\right|\right|^2}{\sqrt{\left|\left|E_{pi}^{\mathrm{T}} z_{vi}\right|\right|^2+\varepsilon_i^2}} + \tilde{w}_{\mathrm{a}i}^{\mathrm{T}}(H_{\mathrm{a}i}\otimes B_{\mathrm{a}i}) \\
&\quad - \tilde{w}_{\mathrm{a}i}^{\mathrm{T}}\left[(G_{\alpha \mathrm{a}i}^{\mathrm{T}} z_{vi})\otimes B_{\mathrm{a}i}\right] - \tilde{w}_{\mathrm{a}i}^{\mathrm{T}}\left[(\xi_{\mathrm{a}i}^{\mathrm{T}} z_{vi})\otimes B_{\mathrm{a}i}\right] \\
&\quad - \tilde{w}_{\mathrm{a}i}^{\mathrm{T}}\left(E_{\mathrm{a}i}\otimes B_{\mathrm{a}i}\right) z_{si}\frac{\partial v_{\mathrm{d}i}}{\partial d_{\mathrm{a}i}} + (4\bar{\delta}_{\mathrm{a}}+\bar{\delta}_i)\varepsilon_i\Bigg\}.
\end{aligned} \tag{38}$$

Finally, design the adaptive laws for the estimators $\hat{w}_{\mathrm{a}i}$, $\hat{\delta}_{\mathrm{a}i}$, and $\hat{\delta}_i$ $(i = 1, \cdots, N)$ as the following

$$\dot{\hat{w}}_{\mathrm{a}i} = n_{w\mathrm{a}i}\Bigg(-(H_{\mathrm{a}i}\otimes B_{\mathrm{a}i}) + (G_{\alpha \mathrm{a}i}^{\mathrm{T}} z_{vi})\otimes B_{\mathrm{a}i} + (\xi_{\mathrm{a}i}^{\mathrm{T}} z_{vi})\otimes B_{\mathrm{a}i} + (E_{\mathrm{a}i}\otimes B_{\mathrm{a}i}) z_{si}\frac{\partial v_{\mathrm{d}i}}{\partial d_{\mathrm{a}i}}\Bigg) - \sigma_{w\mathrm{a}i}\hat{w}_{\mathrm{a}i}, \tag{39}$$

$$\dot{\hat{\delta}}_{\mathrm{a}i} = n_{\delta \mathrm{a}i}\Bigg(\frac{||H_{\mathrm{a}i}||^2}{\sqrt{||H_{\mathrm{a}i}||^2+\varepsilon_i^2}} + \frac{\left|\left|\xi_{\mathrm{a}i}^{\mathrm{T}} z_{vi}\right|\right|^2}{\sqrt{\left|\left|\xi_{\mathrm{a}i}^{\mathrm{T}} z_{vi}\right|\right|^2+\varepsilon_i^2}} + \frac{\left|\left|G_{\alpha \mathrm{a}i}^{\mathrm{T}} z_{vi}\right|\right|^2}{\sqrt{\left|\left|G_{\alpha \mathrm{a}i}^{\mathrm{T}} z_{vi}\right|\right|^2+\varepsilon_i^2}} + \frac{z_{si}^2\left|\left|\frac{\partial v_{\mathrm{d}i}}{\partial d_{\mathrm{a}i}} E_{\mathrm{a}i}\right|\right|^2}{\sqrt{z_{si}^2\left|\left|\frac{\partial v_{\mathrm{d}i}}{\partial d_{\mathrm{a}i}} E_{\mathrm{a}i}\right|\right|^2+\varepsilon_i^2}}\Bigg) - \sigma_{\delta \mathrm{a}i}\hat{\delta}_{\mathrm{a}i}, \tag{40}$$

$$\dot{\hat{\delta}}_i = n_{\delta i}\frac{\left|\left|E_{pi}^{\mathrm{T}} z_{vi}\right|\right|^2}{\sqrt{\left|\left|E_{pi}^{\mathrm{T}} z_{vi}\right|\right|^2+\varepsilon_i^2}} - \sigma_{\delta i}\hat{\delta}_i, \tag{41}$$

where $\hat{w}_{\mathrm{a}i}(0) = \hat{w}_{\mathrm{a}i0}$, $\hat{\delta}_{\mathrm{a}i}(0) = \hat{\delta}_{\mathrm{a}i0}$, and $\hat{\delta}_i(0) = \hat{\delta}_{i0}$, with $\hat{w}_{\mathrm{a}i0}$, $\hat{\delta}_{\mathrm{a}i0}$, and $\hat{\delta}_{i0}$ being the initial conditions. $n_{w\mathrm{a}i}$, $n_{\delta \mathrm{a}i}$, $n_{\delta i}$, $\sigma_{w\mathrm{a}i}$, $\sigma_{\delta \mathrm{a}i}$, and $\sigma_{\delta i}$ are positive design constants. Design the Lyapunov function candidates for the estimators as $V_{w\mathrm{a}} = \sum_{i=1}^{N}\frac{1}{2n_{w\mathrm{a}i}}\tilde{w}_{\mathrm{a}i}^{\mathrm{T}}\tilde{w}_{\mathrm{a}i}$, $V_{\delta \mathrm{a}} = \sum_{i=1}^{N}\frac{1}{2n_{\delta \mathrm{a}i}}\tilde{\delta}_{\mathrm{a}i}^2$, and $V_\delta = \sum_{i=1}^{N}\frac{1}{2n_{\delta i}}\tilde{\delta}_i^2$.

Denote $V_{\mathrm{pos}} = V_1 + V_2 + V_s + V_{w\mathrm{a}} + V_{\delta \mathrm{a}} + V_\delta$, for its time derivative we can get $\dot{V}_{\mathrm{pos}} < \sum_{i=1}^{N}\Big(-K_{\mathrm{e}i}\eta_{\mathrm{e}i}^2 - K_{\mathrm{a}i}\eta_{\mathrm{a}i}^2 - \sum_{j\in\mathcal{N}_i} K_{\mathrm{e}ij}\eta_{\mathrm{e}ij}^2 - K_{vi} z_{vi}^{\mathrm{T}} z_{vi} - K_{si} z_{si}^2 - \frac{\sigma_{w\mathrm{a}i}}{2n_{w\mathrm{a}i}}\tilde{w}_{\mathrm{a}i}^{\mathrm{T}}\tilde{w}_{\mathrm{a}i} - \frac{\sigma_{\delta \mathrm{a}i}}{2n_{\delta \mathrm{a}i}}\tilde{\delta}_{\mathrm{a}i}^2 - \frac{\sigma_{\delta i}}{2n_{\delta i}}\tilde{\delta}_i^2 + c_{1i}\Big)$, where $c_{1i} = \frac{\sigma_{w\mathrm{a}i}}{2n_{w\mathrm{a}i}} w_{\mathrm{a}}^{\mathrm{T}} w_{\mathrm{a}} + \frac{\sigma_{\delta \mathrm{a}i}}{2n_{\delta \mathrm{a}i}}\bar{\delta}_{\mathrm{a}}^2 + \frac{\sigma_{\delta i}}{2n_{\delta i}}\bar{\delta}_i^2 + (4\bar{\delta}_{\mathrm{a}} + \bar{\delta}_i)\varepsilon_i$ $(i = 1, \cdots, N)$. Hence,

$$\dot{V}_{\mathrm{pos}} < -\kappa_1 V_{\mathrm{pos}} + \varrho_1, \tag{42}$$

where $\kappa_1 \triangleq \min_{i,\ j\in\mathcal{N}_i}(2K_{\mathrm{e}i}, 2K_{\mathrm{a}i}, 2K_{\mathrm{e}ij}, 2K_{vi}, 2K_{si}, \sigma_{w\mathrm{a}i}, \sigma_{\delta \mathrm{a}i}, \sigma_{\delta i})$, $\varrho_1 \triangleq \sum_{i=1}^{N} c_{1i}$. The aforementioned design procedure leads to the following theoretical result.

Theorem 3.1: With the thrust laws (33) and (34), adaptive laws (39), (40), and (41), and the path parameter timing law (37), the quadrotor team described by (1) under Assumptions 2.1-2.5 will have the following results:

i) The environment-aware dynamic constraint requirements (13), (14), and (16) will be met during formation.

ii) The transformed output tracking errors $\eta_{\mathrm{e}i}$ and $\eta_{\mathrm{e}ij}$ $(i = 1, \cdots, N,\ j \in \mathcal{N}_i)$ will converge into the set

$$\left\{x = \eta_{\mathrm{e}i}, \eta_{\mathrm{e}ij} \ : \ |x| < \varepsilon_\eta, \quad \varepsilon_\eta = \sqrt{\frac{2\varrho_1}{\kappa_1}}\right\}, \tag{43}$$

which implies that the output tracking errors $d_{\mathrm{e}i}$ and $d_{\mathrm{e}ij}$ will converge into the following regions

$$\left\{d_{\mathrm{e}i} : \max(\varepsilon_{\mathrm{e}i}, 2\varepsilon_{\mathrm{e}i} + \varepsilon_{\chi_{\mathrm{L}i}}) < d_{\mathrm{e}i} < 2\varepsilon_{\mathrm{e}i} + \varepsilon_{\chi_{\mathrm{H}i}}\right\}, \tag{44}$$

$$\left\{d_{\mathrm{e}ij} : -\varepsilon_{\iota_{\mathrm{L}ij}} < d_{\mathrm{e}ij} < \varepsilon_{\iota_{\mathrm{H}ij}}\right\}, \tag{45}$$

where $\varepsilon_{\chi_{\mathrm{H}i}}$ and $\varepsilon_{\chi_{\mathrm{L}i}}$ are expressed as

$$\varepsilon_{\chi_{\mathrm{H}i}} = \frac{\left\{\begin{matrix}[\varepsilon_\eta(\Omega_{d\mathrm{H}i} - \varepsilon_{\mathrm{e}i}) - \Omega_{d\mathrm{H}i}] \\ + \sqrt{[\varepsilon_\eta(\Omega_{d\mathrm{H}i} - \varepsilon_{\mathrm{e}i}) - \Omega_{d\mathrm{H}i}]^2 + 4\varepsilon_\eta^2\Omega_{d\mathrm{H}i}\varepsilon_{\mathrm{e}i}}\end{matrix}\right\}}{2\varepsilon_\eta},$$

$$\varepsilon_{\chi_{\mathrm{L}i}} = \frac{\left\{\begin{matrix}[\varepsilon_\eta(\Omega_{d\mathrm{H}i} - \varepsilon_{\mathrm{e}i}) + \Omega_{d\mathrm{H}i}] \\ - \sqrt{[\varepsilon_\eta(\Omega_{d\mathrm{H}i} - \varepsilon_{\mathrm{e}i}) + \Omega_{d\mathrm{H}i}]^2 + 4\varepsilon_\eta^2\Omega_{d\mathrm{H}i}\varepsilon_{\mathrm{e}i}}\end{matrix}\right\}}{2\varepsilon_\eta}.$$

Moreover, $\varepsilon_{\iota_{\mathrm{H}ij}}$ and $\varepsilon_{\iota_{\mathrm{L}ij}}$ can be written as

$$\varepsilon_{\iota_{\mathrm{H}ij}} = \frac{\left(\begin{array}{l} -(\Omega_{\mathrm{H}ij}\Omega_{\mathrm{L}ij} - \varepsilon_\eta(\Omega_{\mathrm{H}ij} - \Omega_{\mathrm{L}ij})) \\ \quad + \sqrt{\Omega_{\mathrm{H}ij}^2\Omega_{\mathrm{L}ij}^2 + \varepsilon_\eta^2(\Omega_{\mathrm{H}ij} + \Omega_{\mathrm{L}ij})^2 \\ \qquad - 2\varepsilon_\eta\Omega_{\mathrm{H}ij}\Omega_{\mathrm{L}ij}(\Omega_{\mathrm{H}ij} - \Omega_{\mathrm{L}ij})} \end{array}\right)}{2\varepsilon_\eta},$$

$$\varepsilon_{\iota_{\mathrm{L}ij}} = \frac{\left(\begin{array}{l} -(\Omega_{\mathrm{H}ij}\Omega_{\mathrm{L}ij} + \varepsilon_\eta(\Omega_{\mathrm{H}ij} - \Omega_{\mathrm{L}ij})) \\ \quad + \sqrt{\Omega_{\mathrm{H}ij}^2\Omega_{\mathrm{L}ij}^2 + \varepsilon_\eta^2(\Omega_{\mathrm{H}ij} + \Omega_{\mathrm{L}ij})^2 \\ \qquad + 2\varepsilon_\eta\Omega_{\mathrm{H}ij}\Omega_{\mathrm{L}ij}(\Omega_{\mathrm{H}ij} - \Omega_{\mathrm{L}ij})} \end{array}\right)}{2\varepsilon_\eta}.$$

iii) For each quadrotor, the path speed error $z_{si}(t) = \dot{s}_i(t) - v_{\mathrm{d}i}(s_i(t), d_{\mathrm{a}i}(t))$ satisfies $\limsup_{t\to\infty} |\dot{s}_i(t) - v_{\mathrm{d}i}(s_i(t), d_{\mathrm{a}i}(t))| < \varepsilon_\eta$.

iv) The adaptive laws (39), (40), and (41), and the path parameter timing law (37), are all uniformly bounded.

Proof: From (42) we have

$$V_{\mathrm{pos}}(t) < \Big(V_{\mathrm{pos}}(0) - \frac{\varrho_1}{\kappa_1}\Big)e^{-\kappa_1 t} + \frac{\varrho_1}{\kappa_1}. \tag{46}$$

The boundedness of V_{pos} implies boundedness of $\eta_{\mathrm{e}i}$, $\eta_{\mathrm{a}i}$, and $\eta_{\mathrm{e}ij}$ ($i = 1, \cdots, N$, $j \in \mathcal{N}_i$). Hence, the constraint requirements (13), (14), and (16) are satisfied during the operation.

Moreover, we have $\limsup_{t\to\infty} V_{\mathrm{pos}} < \frac{\varrho_1}{\kappa_1}$, hence $\frac{1}{2}\eta_{\mathrm{e}i}^2 < \frac{\varrho_1}{\kappa_1}$ when $t \to \infty$, therefore $\eta_{\mathrm{e}i}$ will converge to the set (43). Similar relationship holds for $\eta_{\mathrm{e}ij}$. Furthermore, uniform boundedness of V_{pos} implies boundedness of adaptive estimates $\hat{w}_{\mathrm{a}i}$, $\hat{\delta}_{\mathrm{a}i}$, and $\hat{\delta}_i$, as well as fictitious errors z_{vi}.

Next, note that in the range $-\varepsilon_{\mathrm{e}i} < d_{\varepsilon\mathrm{e}i} < \Omega_{d\mathrm{H}i}$, $\eta_{\mathrm{e}i}$ is a function in $d_{\varepsilon\mathrm{e}i}$. Recall that $d_{\varepsilon\mathrm{e}i} \triangleq d_{\mathrm{e}i} - 2\varepsilon_{\mathrm{e}i}$, with $\varepsilon_{\mathrm{e}i} > 0$ being an arbitrarily small constant. Hence, the range (13) gives the range for $d_{\mathrm{e}i}$ given in (44). Besides, within the range of (16), $\eta_{\mathrm{e}ij}$ is quadratically related to $d_{\mathrm{e}ij}$. Hence, satisfying the constraints (13), (14), and (16) means that the distance tracking errors $d_{\mathrm{e}i}$ and $d_{\mathrm{e}ij}$ will be confined in the ranges defined by (44) and (45).

Furthermore, since $\limsup_{t\to\infty} \frac{1}{2}z_{si}^2 < \frac{\varrho_1}{\kappa_1}$, the speed assignment error will satisfy $|\dot{s}_i - v_{\mathrm{d}i}| < \varepsilon_\eta$ when $t \to \infty$ for $i = 1, \cdots, N$. Besides, the boundedness of $v_{\mathrm{d}i}$ will lead to the boundedness of $\dot{s}_i(t)$.

Finally, boundedness of the adaptive estimates $\hat{w}_{\mathrm{a}i}$, $\hat{\delta}_{\mathrm{a}i}$, and $\hat{\delta}_i$, the path speed variable s_i, its derivative signal $\dot{s}_i$, and the fictitious error z_{vi} as well as the invertibility of $E_{pi}^{\mathrm{T}}E_{pi}$ imply that α_{pi}, u_i, and u_{i0} are all uniformly bounded. Hence, it is clear to imply that adaptive laws (39), (40), and (41), and the path parameter timing law (37), are all uniformly bounded. ■

Remark 3.5: In Theorem 3.1, using L'Hôpital's rule yields

$$\begin{aligned} &\lim_{\varepsilon_\eta\to 0} \varepsilon_{\chi_{\mathrm{H}i}} = 0, \quad \lim_{\varepsilon_\eta\to 0} \varepsilon_{\chi_{\mathrm{L}i}} = 0, \\ &\lim_{\varepsilon_\eta\to 0} \varepsilon_{\iota_{\mathrm{H}ij}} = 0, \quad \lim_{\varepsilon_\eta\to 0} \varepsilon_{\iota_{\mathrm{L}ij}} = 0, \end{aligned} \tag{47}$$

for $i = 1, \cdots, N$. This implies that when the modified error variables $\eta_{\mathrm{e}i}$ and $\eta_{\mathrm{e}ij}$ converge into small neighborhoods of zero, the relative LOS tracking error $d_{\mathrm{e}ij}$ will converge to a region close to zero and the actual LOS tracking error $d_{\mathrm{e}i}$ will converge to a region arbitrarily close to $2\varepsilon_{\mathrm{e}i}$, with $\varepsilon_{\mathrm{e}i} > 0$ being an arbitrarily small constant.

Remark 3.6: To reduce the set size in (43), we need to select large κ_1 and small ϱ_1. To make κ_1 large, we can select large control gains $K_{\mathrm{e}i}$, $K_{\mathrm{a}i}$, $K_{\mathrm{e}ij}$, and K_{vi} ($i = 1, \cdots, N$, $j \in \mathcal{N}_i$), and large adaptive and path timing law parameters $\sigma_{w\mathrm{a}i}$, $\sigma_{\delta\mathrm{a}i}$, $\sigma_{\delta i}$, and K_{si}. To make ϱ_1 small, we can select small ε_i, and large adaptive parameters $n_{w\mathrm{a}i}$, $n_{\delta\mathrm{a}i}$, and $n_{\delta i}$.

B. Attitude Control Design and Results

Step 3:

Next, we select the Lyapunov function candidate as $V_3 = \sum_{i=1}^N \frac{1}{2}z_{\Theta i}^{\mathrm{T}}z_{\Theta i}$. With some algebraic analysis shown in Appendix C (see (66)–(71)), the stabilizing function $\alpha_{\Theta i} \in \mathbb{R}^3$ for the ith quadrotor ($i = 1, \cdots, N$) is designed as

$$\alpha_{\Theta i} = -\Big(K_{\Theta i} + \frac{\nu_{\Theta i}}{2}\Big)z_{\Theta i}, \tag{48}$$

where $K_{\Theta i} > 0$ is a control gain and $\nu_{\Theta i} > 0$ is a design constant.

Step 4:

At this step, select the Lyapunov function candidate as $V_4 = \sum_{i=1}^N \frac{1}{2}z_{\omega i}^{\mathrm{T}}M_i(\Theta_i)z_{\omega i}$. With some algebraic analysis shown in Appendix D (see (72)–(73)), the torque law for the ith quadrotor ($i = 1, \cdots, N$) is designed as

$$\tau_i = -\frac{\Psi(\Theta_i)z_{\omega i}\left|\left|\bar{\tau}_i\right|\right|^2\hat{\rho}_{Ji}^2}{\sqrt{\left|\left|\Psi(\Theta_i)z_{\omega i}\right|\right|^2\left|\left|\bar{\tau}_i\right|\right|^2\hat{\rho}_{Ji}^2 + \varepsilon_i^2}}, \tag{49}$$

$$\bar{\tau}_i = T^{\mathrm{T}}(\Theta_i)(K_{\omega i}z_{\omega i} + z_{\Theta i}) + \hat{\mu}_{Ji}\frac{T^{\mathrm{T}}(\Theta_i)z_{\omega i}\Xi_i^2}{\sqrt{\left|\left|z_{\omega i}\right|\right|^2\Xi_i^2 + \varepsilon_i^2}}, \tag{50}$$

$$\dot{\hat{\rho}}_{Ji} = n_{\rho Ji}z_{\omega i}^{\mathrm{T}}\Psi^{\mathrm{T}}(\Theta_i)\bar{\tau}_i - \sigma_{\rho Ji}\hat{\rho}_{Ji}, \tag{51}$$

$$\dot{\hat{\mu}}_{Ji} = n_{\mu Ji}\frac{\left|\left|z_{\omega i}\right|\right|^2\Xi_i^2}{\sqrt{\left|\left|z_{\omega i}\right|\right|^2\Xi_i^2 + \varepsilon_i^2}} - \sigma_{\mu Ji}\hat{\mu}_{Ji}, \tag{52}$$

where $\hat{\rho}_{Ji}(0) = \hat{\rho}_{Ji0}$ and $\hat{\mu}_{Ji}(0) = \hat{\mu}_{Ji0}$ are the initial conditions. $K_{\omega i} > 0$ is a positive control gain. Ξ_i is introduced in (73). $\hat{\rho}_{Ji}$ is the adaptive estimate of the unknown constant $\rho_{Ji} = \frac{1}{J_i}$ and $\hat{\mu}_{Ji}$ is the adaptive estimate of the unknown constant $\bar{\mu}_{Ji}$ introduced in (73). $n_{\rho Ji}$, $n_{\mu Ji}$, $\sigma_{\rho Ji}$, and $\sigma_{\mu Ji}$ are positive design constants. Denote

$$\begin{aligned} V_{\mathrm{att}} &= V_3 + V_4 + V_{\rho J} + V_{\mu J}, \\ V_{\rho J} &= \sum_{i=1}^N \frac{J_i}{2n_{\rho Ji}}\tilde{\rho}_{Ji}^2, \quad V_{\mu J} = \sum_{i=1}^N \frac{1}{2n_{\mu Ji}}\tilde{\mu}_{Ji}^2, \end{aligned} \tag{53}$$

where $\tilde{\rho}_{Ji} = \hat{\rho}_{Ji} - \rho_{Ji}$ and $\tilde{\mu}_{Ji} = \hat{\mu}_{Ji} - \bar{\mu}_{Ji}$. After some algebraic manipulation, we can arrive at $\dot{V}_{\mathrm{att}} < \sum_{i=1}^N\big(-K_{\Theta i}z_{\Theta i}^{\mathrm{T}}z_{\Theta i} - K_{\omega i}z_{\omega i}^{\mathrm{T}}z_{\omega i} - \frac{\sigma_{\rho Ji}\underline{J}_i}{2n_{\rho Ji}}\tilde{\rho}_{Ji}^2 - \frac{\sigma_{\mu Ji}}{2n_{\mu Ji}}\tilde{\mu}_{Ji}^2 + c_{2i}\big)$, where $c_{2i} = \varepsilon_i(\underline{J}_i + \bar{\mu}_{Ji}) + \frac{\sigma_{\rho Ji}}{2n_{\rho Ji}}\frac{1}{\underline{J}_i} + \frac{\sigma_{\mu Ji}}{2n_{\mu Ji}}\bar{\mu}_{Ji}^2 + \frac{1}{2\nu_{\Theta i}}\bar{\Theta}_{\mathrm{d}i}^2$ ($i = 1, \cdots, N$). Hence,

$$\dot{V}_{\mathrm{att}} < -\kappa_2 V_{\mathrm{att}} + \varrho_2, \tag{54}$$

where $\kappa_2 \triangleq \min_i\big(2K_{\Theta i}, \frac{2K_{\omega i}}{M_i}, \sigma_{\rho Ji}, \sigma_{\mu Ji}\big)$ and $\varrho_2 = \sum_{i=1}^N c_{2i}$.

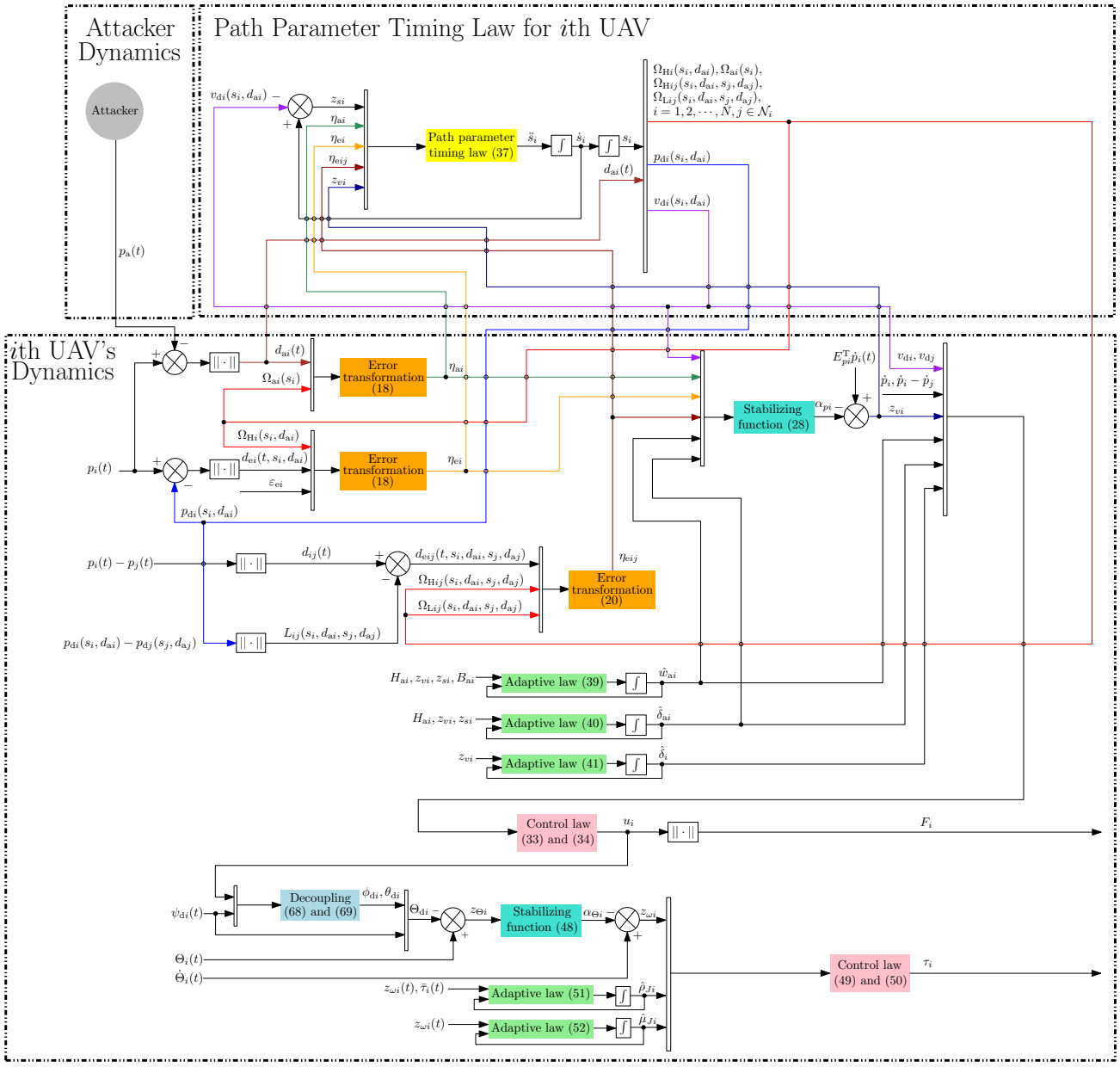

Fig. 2. Block diagram of the overall control algorithm.

The above design leads to the following theoretical result.

Theorem 3.2: With the UAV torque laws (49) and (50), and adaptive laws (51) and (52), the attitude of the quadrotor team described by (2) and (3) under Assumptions 2.1–2.6 has the following properties:

i) The attitude tracking error of the ith quadrotor ($i = 1, \cdots, N$) $z_{\Theta i}$ will converge into the set

$$\left\{ z_{\Theta i} \;\middle|\; ||z_{\Theta i}|| < \varepsilon_\eta,\ \varepsilon_\eta = \sqrt{\frac{2\varrho_2}{\kappa_2}} \right\}, \tag{55}$$

ii) The adaptive laws (51) and (52) are uniformly bounded.

Proof: First of all, (54) leads to

$$V_{\rm att}(t) < \left(V_{\rm att}(0) - \frac{\varrho_2}{\kappa_2} \right) e^{-\kappa_2 t} + \frac{\varrho_2}{\kappa_2}, \tag{56}$$

hence $V_{\rm att}$ is uniformly bounded.

Next, we have $\limsup_{t\to\infty} V_{\rm att} < \frac{\varrho_2}{\kappa_2}$, hence $\frac{1}{2} z_{\Theta i}^2 < \frac{\varrho_2}{\kappa_2}$ when $t \to \infty$, therefore $z_{\Theta i}$ will converge to the set (55). Furthermore, boundedness of the adaptive estimates $\hat{\rho}_{Ji}$ and $\hat{\mu}_{Ji}$, as well as boundedness of the fictitious error $z_{\omega i}$, are now obvious since $V_{\rm att}$ is bounded. Therefore, it is straightforward to prove the boundedness of adaptive laws (51) and (52). ■

Remark 3.7: Our proposed path-dependent constrained adaptive formation control framework, which includes the thrust laws (33) and (34), torques (49) and (50), adaptive laws (39), (40), (41), (51), and (52), and the path parameter timing law (37), is fully distributed since it only requires states of the agent itself, desired path and speed signals, and relative information of neighboring agents. Absolute information of the neighboring agents, such as their position and velocity, is not required in our proposed control algorithm. Such a distributed control framework is practical and implementable for small

UAV systems with limited communication bandwidth.

The overall control algorithm is summarized in Figure 2.

IV. Simulation Studies

We conduct a simulation with a team of $N = 4$ quadrotors in the presence of an attacker. A comparative study with [53] is also discussed. The communication topology is shown in Figure 3. For $i = 1, 2, 3, 4$, the model parameters of the quadrotors are $m_i = 4\text{kg}$, $g = 9.81\text{m/s}^2$, $J_i = \text{diag}[0.109,\ 0.103,\ 0.0625]\text{kg}\cdot\text{m}^2$. Note that the units of the position, attitude, translational and angular velocities are m, rad, m/s, and rad/s, respectively. The attacker velocity is given as $v_{\text{a}}(Z_{\text{a}}) = \big[-0.45 - 0.1\sin(2d_{\text{a1}}) - 0.15\cos(2d_{\text{a2}}) - 0.3\sin(2d_{\text{a3}}) - 0.3\cos(2d_{\text{a4}}),\ 0.55 + 0.1\sin(2d_{\text{a1}}) + 0.15\cos(2d_{\text{a2}}) + 0.3\sin(2d_{\text{a3}}) + 0.3\cos(2d_{\text{a4}}),\ -1.9 - \big(\frac{0.05}{d_{\text{a1}}+1} + \frac{0.05}{d_{\text{a2}}+1} + \frac{0.05}{d_{\text{a3}}+1} + \frac{0.05}{d_{\text{a4}}+1}\big)\big]^{\text{T}}$, which is based on relative distances from the team and unknown for the controller design. The desired paths for agents are given as $p_{\text{d1}}(s_1, d_{\text{a1}}) = \big[0.8\cos(0.4s_1) + 0.15s_1 + \frac{0.3}{d_{\text{a1}}} + 0.6,\ 0.8\sin(0.4s_1) + 0.15s_1 + \frac{0.3}{d_{\text{a1}}} + 0.6,\ -0.4s_1 + \frac{0.3}{d_{\text{a1}}} + 2.5\big]^{\text{T}}$, $p_{\text{d2}}(s_2, d_{\text{a2}}) = \big[0.8\cos(0.4s_2) + 0.15s_2 + \frac{0.3}{d_{\text{a2}}} + 0.6,\ 0.8\sin(0.4s_2) + 0.15s_2 + \frac{0.3}{d_{\text{a2}}} + 1.75,\ -0.4s_2 + \frac{0.3}{d_{\text{a2}}} + 2.5\big]^{\text{T}}$, $p_{\text{d3}}(s_3, d_{\text{a3}}) = \big[0.8\cos(0.4s_3) + 0.15s_3 + \frac{0.3}{d_{\text{a3}}} + 1.75,\ 0.8\sin(0.4s_3) + 0.15s_3 + \frac{0.3}{d_{\text{a3}}} + 0.65,\ -0.4s_3 + \frac{0.3}{d_{\text{a3}}} + 2.5\big]^{\text{T}}$, and $p_{\text{d4}}(s_4, d_{\text{a4}}) = \big[0.8\cos(0.4s_4) + 0.15s_4 + \frac{0.3}{d_{\text{a4}}} + 1.65,\ 0.8\sin(0.4s_4) + 0.15s_4 + \frac{0.3}{d_{\text{a4}}} + 1.65,\ -0.4s_4 + \frac{0.3}{d_{\text{a4}}} + 2.5\big]^{\text{T}}$. The reference yaw signals are selected as $\psi_{\text{di}} = 0$, $i = 1, 2, 3, 4$. The desired speed assignments for quadrotors are chosen as $v_{\text{di}} = 1.5 - \exp(-0.5s_i) + \frac{0.55}{d_{\text{ai}}}$. The safety constraint functions are designed as $\Omega_{\text{ai}}(s_i) = 1.6 - 1.4\exp(-0.3s_i)$, $\Omega_{\text{H}ij}(s_i, d_{\text{ai}}, s_j, d_{\text{aj}}) = 0.3 + 1.5\Big(\frac{\exp(-0.1s_i)+\exp(-0.1s_j)}{2}\Big) - \frac{0.8}{d_{\text{ai}}} - \frac{0.8}{d_{\text{aj}}}$, and $\Omega_{\text{L}ij}(s_i, d_{\text{ai}}, s_j, d_{\text{aj}}) = 0.4 + 1.1\Big(\frac{\exp(-0.15s_i)+\exp(-0.15s_j)}{2}\Big) - \frac{0.3}{d_{\text{ai}}} - \frac{0.3}{d_{\text{aj}}}$, $i = 1, 2, 3, 4$, $j \in \mathcal{N}_i$. The performance constraint functions for quadrotors are selected as $\Omega_{\text{H}i}(s_i, d_{\text{ai}}) = 0.26 + 5.34\exp(-0.15s_i) - \frac{2}{d_{\text{ai}}}$ and the lower bounds are $\varepsilon_{ei} = 0.05$. The external disturbances are $N_{1i} = [0.105\sin(0.2t),\ 0.06\cos(0.05t),\ 0.03\cos(0.12t)]^{\text{T}}$ and $N_{2i} = [0.01\sin(0.14t),\ 0.01\sin(0.14t),\ 0.06\sin(0.3t)]^{\text{T}}$.

The number of neural network nodes is selected as $n = 3$ and the basis functions are given as $b_k(Z_{\text{ai}}) = \exp\Big[-\frac{(Z_{\text{ai}}-\nu_k)^{\text{T}}(Z_{\text{ai}}-\nu_k)}{\zeta_k^2}\Big]$, $k = 1, 2, 3$, $i = 1, 2, 3, 4$. For the basis functions, the width values are given as $\zeta_1 = \zeta_2 = \zeta_3 = 2$ and the receptive field's centers are selected as $\nu_1 = 0.5\cdot\mathbf{1}_9$, $\nu_2 = \mathbf{1}_9$, and $\nu_3 = 1.5\cdot\mathbf{1}_9$, where $\mathbf{1}_9 = [1,\ 1,\ 1,\ 1,\ 1,\ 1,\ 1,\ 1,\ 1]^{\text{T}} \in \mathbb{R}^9$. We choose the design parameters as $n_{wai} = 0.29$, $n_{\delta ai} = 0.35$, $n_{\delta i} = 0.25$, $n_{\rho Ji} = 0.25$, $n_{\mu Ji} = 0.35$, $\sigma_{wai} = 0.025$, $\sigma_{\delta ai} = 0.1$, $\sigma_{\delta i} = 0.05$, $\sigma_{\rho Ji} = 0.1$, $\sigma_{\mu Ji} = 0.1$, and $\varepsilon_i = 0.1$, $i = 1, 2, 3, 4$. The control gains are designed as $K_{ei} = 0.25$, $K_{\text{a}i} = 0.1$, $K_{eij} = 0.02$, $K_{vi} = 2$, $K_{si} = 30$, $K_{\Theta i} = 1.5$, $\nu_{\Theta i} = 0.5$, and $K_{\omega i} = 2$, $i = 1, 2, 3, 4$, $j \in \mathcal{N}_i$. The initial positions of quadrotors and attacker are $p_1(0) = [0.5,\ 0.5,\ 0]^{\text{T}}$, $p_2(0) = [0.5,\ 1.5,\ 0]^{\text{T}}$, $p_3(0) = [1.5,\ 0.5,\ 0]^{\text{T}}$, $p_4(0) = [1.5,\ 1.5,\ 0]^{\text{T}}$, and $p_a(0) = [6,\ 0,\ 10]^{\text{T}}$. The initial attitudes of quadrotors are $\Theta_i(0) = [0,\ 0,\ 0.3]^{\text{T}}$, $i = 1, 2, 3, 4$. The initial conditions of translational and angular velocities of each UAV are zero.

For the artificial potential function (APF)-based controller [53], controller gains and design parameters are $\beta_1 = 0.25$, $\beta_2 = 2$, $K_F = 0.02$, $K_T = 1.6$, $K_o = 3$, $\delta_{ij} = 0.5$, $\delta_{it} = 0.4$, and $\delta_{io} = 1.6$. The model parameters of quadrotors and attacker dynamics are the same as we selected. Besides, external disturbances and initial states of the UAV team and attacker are identical for both controllers. Simulation results can be found in Figures 4-9. The LOS attacker distance $d_{\text{a}i}$ under our proposed controller (M_1) and APF-based controller (M_2) [53] with the safety constraint function $\Omega_{\text{a}i}$, $i = 1, 2, 3, 4$, are shown in Figure 4. It is evident that the attacker distance $d_{\text{a}i}$ never decreases to the level of $\Omega_{\text{a}i}$ when applying our proposed controller (M_1), implying that the safety constraint requirement (14) is not violated, which is not the case with the APF-based controller (M_2) [53]. As we can see in Figure 4, the safety constraint requirement for the third and forth agents are violated when $5 \le t \le 10$. Thus, under our proposed controller, the quadrotor team is capable of collision avoidance with the attacker during the formation operation. It is worth noting that the attacker is approaching the quadrotor team when $0 \le t \le 8$.

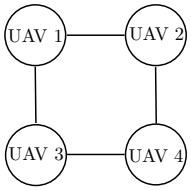

Fig. 3. Undirected communication graph of the UAV team.

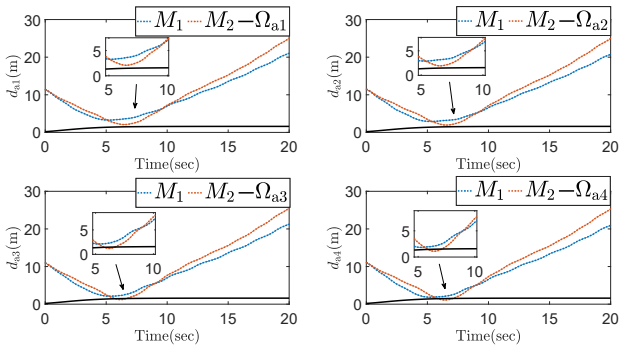

Fig. 4. Comparative simulation results of our proposed controller (M_1) and artificial potential function (APF)-based controller (M_2) [53].

The 3D trajectories of quadrotors and attacker are presented in Figure 5. We can observe that four quadrotors can track their own desired paths without collision with the attacker. Furthermore, when the attacker moves close to the quadrotor group during $0 \le t \le 8$, the desired path for each agent is modified to keep a safe distance from the attacker. The LOS distance tracking errors d_{ei}, $i = 1, 2, 3, 4$, are shown in Figure 6 with higher bounds $\Omega_{\text{H}i}$ and lower bounds ε_{ei}. From this figure, it can be observed that d_{ei} can converge to a small neighborhood of $2\varepsilon_{ei}$ without any violation of the constraint

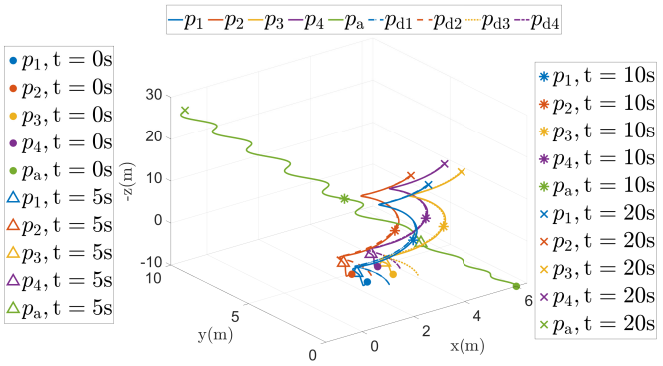

Fig. 5. Trajectories of quadrotors and attacker in 3D space.

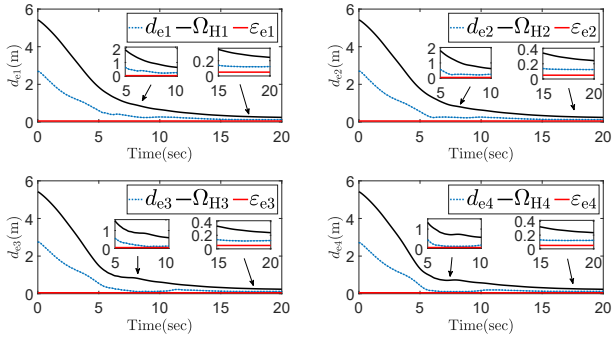

Fig. 6. LOS distance tracking errors profile with performance constraint functions.

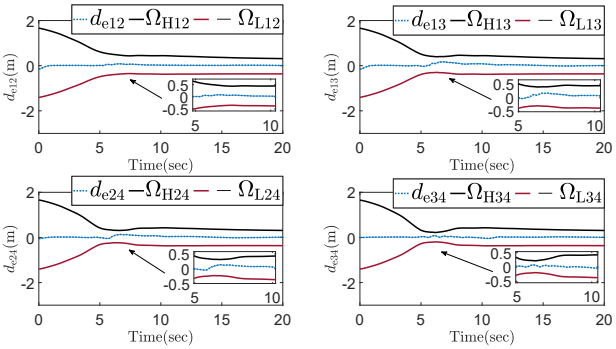

Fig. 7. Inter-quadrotor distance tracking errors profile with safety constraint functions.

requirements, where ε_{ei} can be arbitrarily small positive constants. When $0 \leq t \leq 8$, the performance constraint functions Ω_{Hi} decrease noticeably to make quadrotors get close to their own desired paths, which have been adjusted away from the attacker. Next, Figure 7 gives the profile of inter-quadrotor distance tracking errors d_{eij}, $i = 1, 2, 3, 4$, $j \in \mathcal{N}_i$, from which we can see that safety constraints are never violated, since d_{eij} always stays between the safety constrain functions $-\Omega_{Lij}$ and Ω_{Hij}. When $0 \leq t \leq 8$, a substantial decrease in the path- and attacker-dependent safety constraint functions Ω_{Hij} and Ω_{Lij} can be observed. This reduction enables the UAV team to move towards the modified desired formation in the presence of an approaching attacker. Attitude profiles

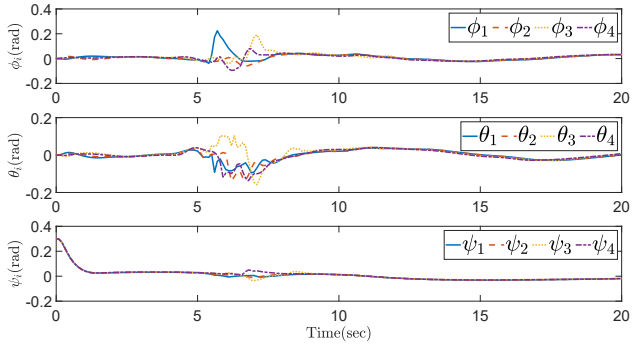

Fig. 8. Attitude profile for quadrotors.

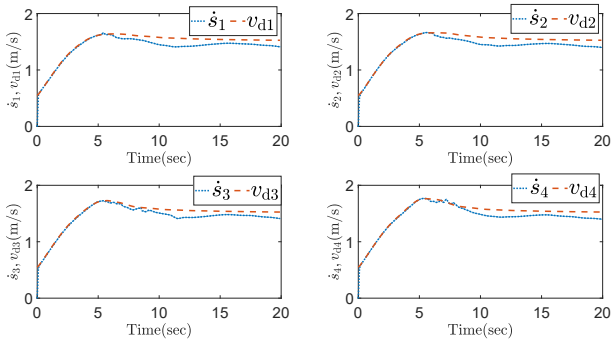

Fig. 9. The profile of path speed $\dot{s}_i$ and desired speed assignment v_{di}, $i = 1, 2, 3, 4$.

for quadrotors are depicted in Figure 8. This figure shows the convergence of the attitudes to their own desired values despite lack of accurate model parameters and the influence of external disturbances. Path speeds $\dot{s}_i$ and desired speed assignments v_{di} are exhibited in Figure 9. During $0 \leq t \leq 8$, when the attacker gets close to the quadrotor group, desired speed assignments v_{di} is able to increase substantially to let each UAV move away from the attacker quickly, and $\dot{s}_i$ can quickly converge to a neighborhood of v_{di}.

Note that in Figure 8, sudden changes of attitudes ϕ_i, θ_i, and ψ_i, and path speeds $\dot{s}_i$ when $5 \leq t \leq 10$ are primarily caused by the attacker being near the quadrotor group. Despite the presence of attacker, quadrotors can rapidly approach their own desired paths p_{di}, which have been adjusted away from the attacker, so that the performance and safety constraint requirements can be guaranteed. From the aforementioned discussion, we can now conclude that the simulation results confirm the theoretic analysis shown in Theorems 3.1 and 3.2.

V. Conclusion

In this work, we developed a formation tracking control architecture for a group of UAVs in the presence of a physical attacker. The safety and performance constraints considered in this work are environment-aware and dynamic in nature, whose formulation depends on certain path parameters and presence of the attacker. The dependence on path ensures adaptation to the dynamic operation environment. The dependence on the attacker ensures that safety/performance

constraints, UAV desired paths, and desired path speeds can be dynamically adjusted, based on the relative distances between the attacker and agents. We also consider path- and attacker-dependent UAV desired paths and desired path speeds. Unknown system parameters and external disturbances are dealt with by adaptive laws. In the future we will look into scenarios where both cyber and physical attacks occur for UAV teams.

ACKNOWLEDGMENT

The authors appreciate the Editor-in-Chief, the Associate Editor, and Reviewers from the IEEE Transactions on Intelligent Vehicles for the helpful comments and constructive suggestions during the review process.

APPENDIX

A. System Dynamics

Denote $\Psi(\Theta_i) = T^{-1}(\Theta_i)$, from (2) we get

$$\omega_i = \Psi(\Theta_i)\dot{\Theta}_i. \tag{57}$$

Hence, multiply J_i^{T} on both sides of (3), and substitute (57) into (3), the angular motion dynamics can be rewritten as

$$\begin{aligned} &J_i^{\mathrm{T}} J_i \Big(\Psi(\Theta_i)\ddot{\Theta}_i + \dot{\Psi}(\Theta_i)\dot{\Theta}_i\Big) \\ &\quad + J_i^{\mathrm{T}}\mathbb{S}\Big(\Psi(\Theta_i)\dot{\Theta}_i\Big) J_i \Psi(\Theta_i)\dot{\Theta}_i = J_i^{\mathrm{T}}\tau_i + J_i^{\mathrm{T}} N_{2i}. \end{aligned} \tag{58}$$

Now, multiply $\Psi^{\mathrm{T}}(\Theta_i)$ on both sides of (58), we can get

$$\begin{aligned} &M_i(\Theta_i)\ddot{\Theta}_i + C_i(\Theta_i, \dot{\Theta}_i)\dot{\Theta}_i \\ &\quad = \Psi^{\mathrm{T}}(\Theta_i) J_i^{\mathrm{T}} \tau_i + \Psi^{\mathrm{T}}(\Theta_i) J_i^{\mathrm{T}} N_{2i}, \end{aligned} \tag{59}$$

where

$$M_i(\Theta_i) = \Psi^{\mathrm{T}}(\Theta_i) J_i^{\mathrm{T}} J_i \Psi(\Theta_i), \tag{60}$$

$$\begin{aligned} C_i(\Theta_i, \dot{\Theta}_i) = &\Psi^{\mathrm{T}}(\Theta_i) J_i^{\mathrm{T}} \mathbb{S}\Big(\Psi(\Theta_i)\dot{\Theta}_i\Big) J_i \Psi(\Theta_i) \\ &+ \Psi^{\mathrm{T}}(\Theta_i) J_i^{\mathrm{T}} J_i \dot{\Psi}(\Theta_i). \end{aligned} \tag{61}$$

It is easy to see $M_i(\Theta_i)$ is symmetric and positive definite, and for any $x \in \mathbb{R}^3$, $x^{\mathrm{T}}\Big(\dot{M}_i(\Theta_i) - 2C_i(\Theta_i, \dot{\Theta}_i)\Big)x = 0$.

B. Step 2 of Backstepping Design

$$\begin{aligned} H_{\alpha \mathrm{a}i} = \Bigg\{ &- \frac{\partial \alpha_{pi}}{\partial(p_i - p_{\mathrm{d}i})}\frac{\partial p_{\mathrm{d}i}}{\partial d_{\mathrm{a}i}} + \frac{\partial \alpha_{pi}}{\partial \Omega_{d\mathrm{H}i}}\frac{\partial \Omega_{d\mathrm{H}i}}{\partial d_{\mathrm{a}i}} \\ &+ \frac{\partial \alpha_{pi}}{\partial(\frac{\partial \Omega_{d\mathrm{H}i}}{\partial s_i})}\frac{\partial^2 \Omega_{d\mathrm{H}i}}{\partial s_i \partial d_{\mathrm{a}i}} + \frac{\partial \alpha_{pi}}{\partial(\frac{\partial \Omega_{d\mathrm{H}i}}{\partial d_{\mathrm{a}i}})}\frac{\partial^2 \Omega_{d\mathrm{H}i}}{\partial d_{\mathrm{a}i}^2} \\ &+ \frac{\partial \alpha_{pi}}{\partial(\frac{\partial p_{\mathrm{d}i}}{\partial s_i})}\frac{\partial^2 p_{\mathrm{d}i}}{\partial s_i \partial d_{\mathrm{a}i}} + \frac{\partial \alpha_{pi}}{\partial(\frac{\partial p_{\mathrm{d}i}}{\partial d_{\mathrm{a}i}})}\frac{\partial^2 p_{\mathrm{d}i}}{\partial d_{\mathrm{a}i}^2} + \frac{\partial \alpha_{pi}}{\partial v_{\mathrm{d}i}}\frac{\partial v_{\mathrm{d}i}}{\partial d_{\mathrm{a}i}} \\ &+ \sum_{j \in \mathcal{N}_i} \Bigg[\frac{\partial \alpha_{pi}}{\partial(p_{\mathrm{d}i} - p_{\mathrm{d}j})}\frac{\partial p_{\mathrm{d}i}}{\partial d_{\mathrm{a}i}} + \frac{\partial \alpha_{pi}}{\partial \Omega_{\mathrm{H}ij}}\frac{\partial \Omega_{\mathrm{H}ij}}{\partial d_{\mathrm{a}i}} \\ &\quad + \frac{\partial \alpha_{pi}}{\partial \Omega_{\mathrm{L}ij}}\frac{\partial \Omega_{\mathrm{L}ij}}{\partial d_{\mathrm{a}i}} + \frac{\partial \alpha_{pi}}{\partial(\frac{\partial \Omega_{\mathrm{H}ij}}{\partial s_i})}\frac{\partial^2 \Omega_{\mathrm{H}ij}}{\partial s_i \partial d_{\mathrm{a}i}} \\ &\quad + \frac{\partial \alpha_{pi}}{\partial(\frac{\partial \Omega_{\mathrm{H}ij}}{\partial d_{\mathrm{a}i}})}\frac{\partial^2 \Omega_{\mathrm{H}ij}}{\partial d_{\mathrm{a}i}^2} + \frac{\partial \alpha_{pi}}{\partial(\frac{\partial \Omega_{\mathrm{L}ij}}{\partial s_i})}\frac{\partial^2 \Omega_{\mathrm{L}ij}}{\partial s_i \partial d_{\mathrm{a}i}} \\ &\quad + \frac{\partial \alpha_{pi}}{\partial(\frac{\partial \Omega_{\mathrm{L}ij}}{\partial d_{\mathrm{a}i}})}\frac{\partial^2 \Omega_{\mathrm{L}ij}}{\partial d_{\mathrm{a}i}^2} \Bigg] \Bigg\} E_{\mathrm{a}i}^{\mathrm{T}} + \frac{\partial \alpha_{pi}}{\partial(p_i - p_{\mathrm{a}})}, \end{aligned} \tag{62}$$

$$\begin{aligned} H_{\alpha \mathrm{a}ij} = \Bigg[&- \frac{\partial \alpha_{pi}}{\partial(p_{\mathrm{d}i} - p_{\mathrm{d}j})}\frac{\partial p_{\mathrm{d}j}}{\partial d_{\mathrm{a}j}} + \frac{\partial \alpha_{pi}}{\partial \Omega_{\mathrm{H}ij}}\frac{\partial \Omega_{\mathrm{H}ij}}{\partial d_{\mathrm{a}j}} \\ &+ \frac{\partial \alpha_{pi}}{\partial \Omega_{\mathrm{L}ij}}\frac{\partial \Omega_{\mathrm{L}ij}}{\partial d_{\mathrm{a}j}} + \frac{\partial \alpha_{pi}}{\partial(\frac{\partial \Omega_{\mathrm{H}ij}}{\partial s_i})}\frac{\partial^2 \Omega_{\mathrm{H}ij}}{\partial s_i \partial d_{\mathrm{a}j}} \\ &+ \frac{\partial \alpha_{pi}}{\partial(\frac{\partial \Omega_{\mathrm{H}ij}}{\partial d_{\mathrm{a}i}})}\frac{\partial^2 \Omega_{\mathrm{H}ij}}{\partial d_{\mathrm{a}i} \partial d_{\mathrm{a}j}} + \frac{\partial \alpha_{pi}}{\partial(\frac{\partial \Omega_{\mathrm{L}ij}}{\partial s_i})}\frac{\partial^2 \Omega_{\mathrm{L}ij}}{\partial s_i \partial d_{\mathrm{a}j}} \\ &+ \frac{\partial \alpha_{pi}}{\partial(\frac{\partial \Omega_{\mathrm{L}ij}}{\partial d_{\mathrm{a}i}})}\frac{\partial^2 \Omega_{\mathrm{L}ij}}{\partial d_{\mathrm{a}i} \partial d_{\mathrm{a}j}} \Bigg] E_{\mathrm{a}j}^{\mathrm{T}} + \frac{\partial \alpha_{pi}}{\partial(p_j - p_{\mathrm{a}})}, \end{aligned} \tag{63}$$

$$\begin{aligned} h_{\alpha si} = &- \frac{\partial \alpha_{pi}}{\partial(p_i - p_{\mathrm{d}i})}\frac{\partial p_{\mathrm{d}i}}{\partial s_i} + \frac{\partial \alpha_{pi}}{\partial \Omega_{d\mathrm{H}i}}\frac{\partial \Omega_{d\mathrm{H}i}}{\partial s_i} + \frac{\partial \alpha_{pi}}{\partial \Omega_{\mathrm{a}i}}\frac{\mathrm{d}\Omega_{\mathrm{a}i}}{\mathrm{d}s_i} \\ &+ \frac{\partial \alpha_{pi}}{\partial(\frac{\partial \Omega_{d\mathrm{H}i}}{\partial s_i})}\frac{\partial^2 \Omega_{d\mathrm{H}i}}{\partial s_i^2} + \frac{\partial \alpha_{pi}}{\partial(\frac{\partial \Omega_{d\mathrm{H}i}}{\partial d_{\mathrm{a}i}})}\frac{\partial^2 \Omega_{d\mathrm{H}i}}{\partial d_{\mathrm{a}i} \partial s_i} \\ &+ \frac{\partial \alpha_{pi}}{\partial(\frac{\mathrm{d}\Omega_{\mathrm{a}i}}{\mathrm{d}s_i})}\frac{\mathrm{d}^2 \Omega_{\mathrm{a}i}}{\mathrm{d}s_i^2} + \frac{\partial \alpha_{pi}}{\partial(\frac{\partial p_{\mathrm{d}i}}{\partial s_i})}\frac{\partial^2 p_{\mathrm{d}i}}{\partial s_i^2} \\ &+ \frac{\partial \alpha_{pi}}{\partial(\frac{\partial p_{\mathrm{d}i}}{\partial d_{\mathrm{a}i}})}\frac{\partial^2 p_{\mathrm{d}i}}{\partial d_{\mathrm{a}i} \partial s_i} + \frac{\partial \alpha_{pi}}{\partial v_{\mathrm{d}i}}\frac{\partial v_{\mathrm{d}i}}{\partial s_i} \\ &+ \sum_{j \in \mathcal{N}_i} \Bigg[\frac{\partial \alpha_{pi}}{\partial(p_{\mathrm{d}i} - p_{\mathrm{d}j})}\frac{\partial p_{\mathrm{d}i}}{\partial s_i} + \frac{\partial \alpha_{pi}}{\partial \Omega_{\mathrm{H}ij}}\frac{\partial \Omega_{\mathrm{H}ij}}{\partial s_i} \\ &\quad + \frac{\partial \alpha_{pi}}{\partial \Omega_{\mathrm{L}ij}}\frac{\partial \Omega_{\mathrm{L}ij}}{\partial s_i} + \frac{\partial \alpha_{pi}}{\partial(\frac{\partial \Omega_{\mathrm{H}ij}}{\partial s_i})}\frac{\partial^2 \Omega_{\mathrm{H}ij}}{\partial s_i^2} \\ &\quad + \frac{\partial \alpha_{pi}}{\partial(\frac{\partial \Omega_{\mathrm{H}ij}}{\partial d_{\mathrm{a}i}})}\frac{\partial^2 \Omega_{\mathrm{H}ij}}{\partial d_{\mathrm{a}i} \partial s_i} + \frac{\partial \alpha_{pi}}{\partial(\frac{\partial \Omega_{\mathrm{L}ij}}{\partial s_i})}\frac{\partial^2 \Omega_{\mathrm{L}ij}}{\partial s_i^2} \\ &\quad + \frac{\partial \alpha_{pi}}{\partial(\frac{\partial \Omega_{\mathrm{L}ij}}{\partial d_{\mathrm{a}i}})}\frac{\partial^2 \Omega_{\mathrm{L}ij}}{\partial d_{\mathrm{a}i} \partial s_i} \Bigg], \end{aligned} \tag{64}$$

$$\begin{aligned} h_{\alpha sij} = &- \frac{\partial \alpha_{pi}}{\partial(p_{\mathrm{d}i} - p_{\mathrm{d}j})}\frac{\partial p_{\mathrm{d}j}}{\partial s_j} + \frac{\partial \alpha_{pi}}{\partial \Omega_{\mathrm{H}ij}}\frac{\partial \Omega_{\mathrm{H}ij}}{\partial s_j} \\ &+ \frac{\partial \alpha_{pi}}{\partial \Omega_{\mathrm{L}ij}}\frac{\partial \Omega_{\mathrm{L}ij}}{\partial s_j} + \frac{\partial \alpha_{pi}}{\partial(\frac{\partial \Omega_{\mathrm{H}ij}}{\partial s_i})}\frac{\partial^2 \Omega_{\mathrm{H}ij}}{\partial s_i \partial s_j} \\ &+ \frac{\partial \alpha_{pi}}{\partial(\frac{\partial \Omega_{\mathrm{H}ij}}{\partial d_{\mathrm{a}i}})}\frac{\partial^2 \Omega_{\mathrm{H}ij}}{\partial d_{\mathrm{a}i} \partial s_j} + \frac{\partial \alpha_{pi}}{\partial(\frac{\partial \Omega_{\mathrm{L}ij}}{\partial s_i})}\frac{\partial^2 \Omega_{\mathrm{L}ij}}{\partial s_i \partial s_j} \\ &+ \frac{\partial \alpha_{pi}}{\partial(\frac{\partial \Omega_{\mathrm{L}ij}}{\partial d_{\mathrm{a}i}})}\frac{\partial^2 \Omega_{\mathrm{L}ij}}{\partial d_{\mathrm{a}i} \partial s_j}. \end{aligned} \tag{65}$$

C. Step 3 of Backstepping Design

Recall that $u_i = F_i R_{\mathrm{d}i} e_z$, we have

$$u_i = F_i \begin{bmatrix} \mathrm{c}\phi_{\mathrm{d}i}\mathrm{s}\theta_{\mathrm{d}i}\mathrm{c}\psi_{\mathrm{d}i} + \mathrm{s}\phi_{\mathrm{d}i}\mathrm{s}\psi_{\mathrm{d}i} \\ \mathrm{c}\phi_{\mathrm{d}i}\mathrm{s}\theta_{\mathrm{d}i}\mathrm{s}\psi_{\mathrm{d}i} - \mathrm{s}\phi_{\mathrm{d}i}\mathrm{c}\psi_{\mathrm{d}i} \\ \mathrm{c}\phi_{\mathrm{d}i}\mathrm{c}\theta_{\mathrm{d}i} \end{bmatrix}, \tag{66}$$

in which we recall that F_i is the thrust of the ith quadrotor. Here, for any designated reference yaw signal $\psi_{\mathrm{d}i}$ satisfying Assumption 2.2, we define ([38])

$$F_i = ||u_i||, \tag{67}$$

$$\phi_{\mathrm{d}i} = \arcsin\Big(\frac{u_{i1}\mathrm{s}\psi_{\mathrm{d}i} - u_{i2}\mathrm{c}\psi_{\mathrm{d}i}}{||u_i||}\Big), \tag{68}$$

$$\theta_{\mathrm{d}i} = \arctan\Big(\frac{u_{i1}\mathrm{c}\psi_{\mathrm{d}i} + u_{i2}\mathrm{s}\psi_{\mathrm{d}i}}{u_{i3}}\Big), \tag{69}$$

where $u_i = [u_{i1},\ u_{i2},\ u_{i3}]^{\mathrm{T}} \in \mathbb{R}^3$, with $\phi_{\mathrm{d}i}$ and $\theta_{\mathrm{d}i}$ satisfying Assumption 2.2.

Choose $V_3 = \sum_{i=1}^{N} \frac{1}{2} z_{\Theta i}^{\mathrm{T}} z_{\Theta i}$ as the Lyapunov function candidate, which has the following time derivative

$$\dot{V}_3 = \sum_{i=1}^{N} z_{\Theta i}^{\mathrm{T}}(z_{\omega i} + \alpha_{\Theta i} - \dot{\Theta}_{\mathrm{d}i}), \tag{70}$$

where we define $z_{\omega i} = \dot{\Theta}_i - \alpha_{\Theta i}$ $(i = 1, \cdots, N)$, with the stabilizing function $\alpha_{\Theta i} \in \mathbb{R}^3$ designed in (48). Taking derivative of $\phi_{\mathrm{d}i}$ in (68) and $\theta_{\mathrm{d}i}$ in (69) with respect to time yields $\dot{\phi}_{\mathrm{d}i} = \frac{\partial \phi_{\mathrm{d}i}}{\partial u_i}\dot{u}_i + \frac{\partial \phi_{\mathrm{d}i}}{\partial \psi_{\mathrm{d}i}}\dot{\psi}_{\mathrm{d}i}$, $\dot{\theta}_{\mathrm{d}i} = \frac{\partial \theta_{\mathrm{d}i}}{\partial u_i}\dot{u}_i + \frac{\partial \theta_{\mathrm{d}i}}{\partial \psi_{\mathrm{d}i}}\dot{\psi}_{\mathrm{d}i}$, where $\psi_{\mathrm{d}i}$ and $\dot{\psi}_{\mathrm{d}i}$ are bounded according to Theorem 3.1 and Assumption 2.2, such that terms $\frac{\partial \phi_{\mathrm{d}i}}{\partial u_i}$, $\frac{\partial \phi_{\mathrm{d}i}}{\partial \psi_{\mathrm{d}i}}$, $\frac{\partial \theta_{\mathrm{d}i}}{\partial u_i}$, and $\frac{\partial \theta_{\mathrm{d}i}}{\partial \psi_{\mathrm{d}i}}$ are all bounded. The result of differentiating u_i in (33) with respect to time can be combined with Theorem 3.1 to conclude the boundedness of $\dot{u}_i$. Therefore, $\dot{\Theta}_{\mathrm{d}i}$ is bounded, which satisfies $\left|\left|\dot{\Theta}_{\mathrm{d}i}\right|\right| < \bar{\Theta}_{\mathrm{d}i}$, where $\bar{\Theta}_{\mathrm{d}i}$ is an unknown positive constant. Note that for any $\nu_{\Theta i} > 0$, $z_{\Theta i}^{\mathrm{T}}\dot{\Theta}_{\mathrm{d}i} < ||z_{\Theta i}||\,\bar{\Theta}_{\mathrm{d}i} \leq \frac{1}{2\nu_{\Theta i}}\bar{\Theta}_{\mathrm{d}i}^2 + \frac{\nu_{\Theta i}}{2}||z_{\Theta i}||^2$. Therefore, from (70) we can get

$$\dot{V}_3 < \sum_{i=1}^{N}\Big(-K_{\Theta i} z_{\Theta i}^{\mathrm{T}} z_{\Theta i} + z_{\Theta i}^{\mathrm{T}} z_{\omega i} + \frac{1}{2\nu_{\Theta i}}\bar{\Theta}_{\mathrm{d}i}^2\Big). \tag{71}$$

D. Step 4 of Backstepping Design

Taking derivative of V_4 yields

$$\dot{V}_4 = \sum_{i=1}^{N} z_{\omega i}^{\mathrm{T}}\Big(\Psi^{\mathrm{T}}(\Theta_i)J_i^{\mathrm{T}}\tau_i + \Psi^{\mathrm{T}}(\Theta_i)J_i^{\mathrm{T}}N_{2i} - M_i(\Theta_i)\dot{\alpha}_{\Theta i} - C_i(\Theta_i, \dot{\Theta}_i)\alpha_{\Theta i}\Big), \tag{72}$$

where, for the term $z_{\omega i}^{\mathrm{T}}\big(\Psi^{\mathrm{T}}(\Theta_i)J_i^{\mathrm{T}}N_{2i} - M_i(\Theta_i)\dot{\alpha}_{\Theta i} - C_i(\Theta_i, \dot{\Theta}_i)\alpha_{\Theta i}\big)$, we can get

$$\begin{aligned}
&z_{\omega i}^{\mathrm{T}}\Big(\Psi^{\mathrm{T}}(\Theta_i)J_i^{\mathrm{T}}N_{2i} - M_i(\Theta_i)\dot{\alpha}_{\Theta i} - C_i(\Theta_i, \dot{\Theta}_i)\alpha_{\Theta i}\Big)\\
&= -z_{\omega i}^{\mathrm{T}}\Psi^{\mathrm{T}}(\Theta_i)J_i^{\mathrm{T}}J_i\Big(\dot{\Psi}(\Theta_i)\alpha_{\Theta i}\\
&\quad + \Psi(\Theta_i)(-K_{\Theta i} - \frac{\nu_{\Theta i}}{2})(\dot{\Theta}_i - \dot{\Theta}_{\mathrm{d}i})\Big)\\
&\quad - z_{\omega i}^{\mathrm{T}}\Psi^{\mathrm{T}}(\Theta_i)J_i^{\mathrm{T}}\mathbb{S}(\Psi(\Theta_i)\dot{\Theta}_i)J_i\Psi(\Theta_i)\alpha_{\Theta i}\\
&\quad + z_{\omega i}^{\mathrm{T}}\Psi^{\mathrm{T}}(\Theta_i)J_i^{\mathrm{T}}J_iJ_i^{-1}N_{2i}\\
&\leq ||z_{\omega i}||\,||\Psi(\Theta_i)||\,||J_i||^2\Big(\Big|\Big|\dot{\Psi}(\Theta_i)\alpha_{\Theta i}\Big|\Big| + \Big|\Big|J_i^{-1}N_{2i}\Big|\Big|\\
&\quad + \Big|\Big|\mathbb{S}(\Psi(\Theta_i)\dot{\Theta}_i)\Big|\Big|\,||\Psi(\Theta_i)\alpha_{\Theta i}||\\
&\quad + \bar{\Theta}_{\mathrm{d}i}\Big|\Big|(K_{\Theta i} + \frac{\nu_{\Theta i}}{2})\Psi(\Theta_i)\Big|\Big|\\
&\quad + \Big|\Big|(K_{\Theta i} + \frac{\nu_{\Theta i}}{2})\Psi(\Theta_i)\dot{\Theta}_i\Big|\Big|\Big)\\
&< \varepsilon_i\bar{\mu}_{Ji} + \bar{\mu}_{Ji}\frac{||z_{\omega i}||^2\,\Xi_i^2}{\sqrt{||z_{\omega i}||^2\,\Xi_i^2 + \varepsilon_i^2}},
\end{aligned} \tag{73}$$

where $\bar{\mu}_{Ji}$ is an unknown positive constant such that $||J_i||^2(1 + \bar{\Theta}_{\mathrm{d}i} + \big|\big|J_i^{-1}N_{2i}\big|\big|) \leq \bar{\mu}_{Ji}$ and $\Xi_i \triangleq ||\Psi(\Theta_i)||\Big(\Big|\Big|\dot{\Psi}(\Theta_i)\alpha_{\Theta i}\Big|\Big| + \Big|\Big|(K_{\Theta i} + \frac{\nu_{\Theta i}}{2})\Psi(\Theta_i)\dot{\Theta}_i\Big|\Big| + \Big|\Big|\mathbb{S}(\Psi(\Theta_i)\dot{\Theta}_i)\Big|\Big|\,||\Psi(\Theta_i)\alpha_{\Theta i}|| + \Big|\Big|(K_{\Theta i} + \frac{\nu_{\Theta i}}{2})\Psi(\Theta_i)\Big|\Big| + 1\Big)$ is known.

REFERENCES

[1] T. J. Koo and S. M. Shahruz, "Formation of a group of unmanned aerial vehicles (UAVs)," in *Proc. American Control Conference*, pp. 69–74, 2001.

[2] T. Kopfstedt, M. Mukai, M. Fujita, and C. Ament, "Control of formations of UAVs for surveillance and reconnaissance missions," *IFAC Proceedings Volumes*, vol. 41, no. 2, pp. 5161–5166, 2008.

[3] J. Scherer, S. Yahyanejad, S. Hayat, E. Yanmaz, T. Andre, A. Khan, V. Vukadinovic, C. Bettstetter, H. Hellwagner, and B. Rinner, "An autonomous multi-UAV system for search and rescue," in *Proc. 1st Workshop on Micro Aerial Vehicle Networks, Systems, and Applications for Civilian Use*, pp. 33–38, 2015.

[4] J. Han, Y. Xu, L. Di, and Y. Chen, "Low-cost multi-UAV technologies for contour mapping of nuclear radiation field," *Journal of Intelligent & Robotic Systems*, vol. 70, no. 1-4, pp. 401–410, 2013.

[5] J. Han and Y. Chen, "Multiple UAV formations for cooperative source seeking and contour mapping of a radiative signal field," *Journal of Intelligent & Robotic Systems*, vol. 74, no. 1-2, pp. 323–332, 2014.

[6] J. Zhang, Y. Lu, Y. Wu, C. Wang, D. Zang, A. Abusorrah, and M. Zhou, "PSO-based sparse source location in large-scale environments with a UAV swarm," *IEEE Transactions on Intelligent Transportation Systems*, 2023.

[7] Z. Zhang, X. Peng, and A. Zhang, "Trajectory tracking control for quadrotor slung load system with unknown load's linear velocity and cable length," *IEEE Transactions on Intelligent Vehicles*, 2023. Doi: 10.1109/TIV.2023.3270165.

[8] N. S. Zúñiga, F. Muñoz, M. A. Márquez, E. S. Espinoza, and L. R. G. Carrillo, "Load transportation using single and multiple quadrotor aerial vehicles with swing load attenuation," in *Proc. International Conference on Unmanned Aircraft Systems*, pp. 269–278, 2018.

[9] K. Klausen, C. Meissen, T. I. Fossen, M. Arcak, and T. A. Johansen, "Cooperative control for multirotors transporting an unknown suspended load under environmental disturbances," *IEEE Transactions on Control Systems Technology*, vol. 28, no. 2, pp. 653–660, 2020.

[10] X. Jin and Z. Hu, "Adaptive cooperative load transportation by a team of quadrotors with multiple constraint requirements," *IEEE Transactions on Intelligent Transportation Systems*, vol. 24, no. 1, pp. 801–814, 2023.

[11] A. D. Ames, J. W. Grizzle, and P. Tabuada, "Control barrier function based quadratic programs with application to adaptive cruise control," in *Proc. IEEE Conference on Decision and Control*, pp. 6271–6278, 2014.

[12] X. Xu, P. Tabuada, J. W. Grizzle, and A. D. Ames, "Robustness of control barrier functions for safety critical control," *IFAC-PapersOnLine*, vol. 48, no. 27, pp. 54–61, 2015.

[13] A. D. Ames, X. Xu, J. W. Grizzle, and P. Tabuada, "Control barrier function based quadratic programs for safety critical systems," *IEEE Transactions on Automatic Control*, vol. 62, no. 8, pp. 3861–3876, 2016.

[14] M.-A. Beaudoin and B. Boulet, "Structured learning of safety guarantees for the control of uncertain dynamical systems," *IEEE Transactions on Intelligent Vehicles*, vol. 8, no. 1, pp. 868–877, 2023.

[15] K. P. Tee, S. S. Ge, and E. H. Tay, "Barrier Lyapunov functions for the control of output-constrained nonlinear systems," *Automatica*, vol. 45, no. 4, pp. 918–927, 2009.

[16] B. Ren, S. S. Ge, K. P. Tee, and T. H. Lee, "Adaptive neural control for output feedback nonlinear systems using a barrier Lyapunov function," *IEEE Transactions on Neural Networks*, vol. 21, no. 8, pp. 1339–1345, 2010.

[17] K. P. Tee and S. S. Ge, "Control of nonlinear systems with partial state constraints using a barrier Lyapunov function," *International Journal of Control*, vol. 84, no. 12, pp. 2008–2023, 2011.

[18] Q. Quan, R. Fu, M. Li, D. Wei, Y. Gao, and K.-Y. Cai, "Practical distributed control for VTOL UAVs to pass a virtual tube," *IEEE Transactions on Intelligent Vehicles*, vol. 7, no. 2, pp. 342–353, 2021.

[19] D. Q. Mayne, J. B. Rawlings, C. V. Rao, and P. O. Scokaert, "Constrained model predictive control: Stability and optimality," *Automatica*, vol. 36, no. 6, pp. 789–814, 2000.

[20] S. L. de Oliveira Kothare and M. Morari, "Contractive model predictive control for constrained nonlinear systems," *IEEE Transactions on Automatic Control*, vol. 45, no. 6, pp. 1053–1071, 2000.

[21] X.-B. Hu and W.-H. Chen, "Model predictive control for constrained systems with uncertain state-delays," *International Journal of Robust and Nonlinear Control*, vol. 14, no. 17, pp. 1421–1432, 2004.

[22] D. Q. Mayne, M. M. Seron, and S. Raković, "Robust model predictive control of constrained linear systems with bounded disturbances," *Automatica*, vol. 41, no. 2, pp. 219–224, 2005.

[23] C. Wang, Z. Wang, Z. Zhang, J. Liu, W. Li, Y. Wu, X. Li, H. Yu, and D. Cao, "Integrated post-impact planning and active safety control for autonomous vehicles," *IEEE Transactions on Intelligent Vehicles*, vol. 8, no. 3, pp. 2062–2076, 2023.

[24] D. Ding, Z. Wang, D. W. Ho, and G. Wei, "Observer-based event-triggering consensus control for multiagent systems with lossy sensors and cyber-attacks," *IEEE Transactions on Cybernetics*, vol. 47, no. 8, pp. 1936–1947, 2016.

[25] X. Jin, W. M. Haddad, Z.-P. Jiang, A. Kanellopoulos, and K. G. Vamvoudakis, "An adaptive learning and control architecture for mitigating sensor and actuator attacks in connected autonomous vehicle platoons," *International Journal of Adaptive Control and Signal Processing*, vol. 33, no. 12, pp. 1788–1802, 2019.

[26] W. He, W. Xu, X. Ge, Q.-L. Han, W. Du, and F. Qian, "Secure control of multiagent systems against malicious attacks: A brief survey," *IEEE Transactions on Industrial Informatics*, vol. 18, no. 6, pp. 3595–3608, 2021.

[27] X.-G. Guo, P.-M. Liu, J.-L. Wang, and C. K. Ahn, "Event-triggered adaptive fault-tolerant pinning control for cluster consensus of heterogeneous nonlinear multi-agent systems under aperiodic DoS attacks," *IEEE Transactions on Network Science and Engineering*, vol. 8, no. 2, pp. 1941–1956, 2021.

[28] T. Yin, Z. Gu, and J. H. Park, "Event-based intermittent formation control of multi-UAV systems under deception attacks," *IEEE Transactions on Neural Networks and Learning Systems*, 2022.

[29] X. Gong, M. V. Basin, Z. Feng, T. Huang, and Y. Cui, "Resilient time-varying formation-tracking of multi-UAV systems against composite attacks: A two-layered framework," *IEEE/CAA Journal of Automatica Sinica*, vol. 10, no. 4, pp. 969–984, 2023.

[30] X. Jin, S.-L. Dai, and J. Liang, "Fixed-time path-following control of an autonomous vehicle with path-dependent performance and feasibility constraints," *IEEE Transactions on Intelligent Vehicles*, 2021. Doi: 10.1109/TIV.2021.3119989.

[31] E. Fiorelli, P. Bhatta, N. E. Leonard, and I. Shulman, "Adaptive sampling using feedback control of an autonomous underwater glider fleet," in *Proc. of 13th Int. Symp. on Unmanned Untethered Submersible Technology*, pp. 1–16, 2003.

[32] P. Ogren, E. Fiorelli, and N. E. Leonard, "Cooperative control of mobile sensor networks: Adaptive gradient climbing in a distributed environment," *IEEE Transactions on Automatic control*, vol. 49, no. 8, pp. 1292–1302, 2004.

[33] E. Fiorelli, N. E. Leonard, P. Bhatta, D. A. Paley, R. Bachmayer, and D. M. Fratantoni, "Multi-AUV control and adaptive sampling in monterey bay," *IEEE Journal of Oceanic Engineering*, vol. 31, no. 4, pp. 935–948, 2006.

[34] K. D. Do, Z.-P. Jiang, and J. Pan, "Robust adaptive path following of underactuated ships," *Automatica*, vol. 40, no. 6, pp. 929–944, 2004.

[35] X. Jin, "Fault-tolerant iterative learning control for mobile robots non-repetitive trajectory tracking with output constraints," *Automatica*, vol. 94, pp. 63–71, 2018.

[36] S.-L. Dai, S. He, M. Wang, and C. Yuan, "Adaptive neural control of underactuated surface vessels with prescribed performance guarantees," *IEEE Transactions on Neural Networks and Learning Systems*, vol. 30, no. 12, pp. 3686–3698, 2018.

[37] W. Xie, W. Zhang, and C. Silvestre, "Saturated backstepping-based tracking control of a quadrotor with uncertain vehicle parameters and external disturbances," *IEEE Control Systems Letters*, vol. 6, pp. 1634–1639, 2022.

[38] Z. Zuo and C. Wang, "Adaptive trajectory tracking control of output constrained multi-rotors systems," *IET Control Theory & Applications*, vol. 8, no. 13, pp. 1163–1174, 2014.

[39] C. Wang and Y. Lin, "Decentralized adaptive tracking control for a class of interconnected nonlinear time-varying systems," *Automatica*, vol. 54, pp. 16–24, 2015.

[40] D. Bernstein, "Matrix mathematics: Theory, facts, and formulas," *Princeton University Press*, 2003.

[41] A. G. Bors and I. Pitas, "Median radial basis function neural network," *IEEE Transactions on Neural Networks*, vol. 7, no. 6, pp. 1351–1364, 1996.

[42] H. Simon, "Neural networks: a comprehensive foundation," *Prentice Hall*, 1999.

[43] R. J. Schilling, J. J. Carroll, and A. F. Al-Ajlouni, "Approximation of nonlinear systems with radial basis function neural networks," *IEEE Transactions on Neural Networks*, vol. 12, no. 1, pp. 1–15, 2001.

[44] Y. Li, S. Qiang, X. Zhuang, and O. Kaynak, "Robust and adaptive backstepping control for nonlinear systems using RBF neural networks," *IEEE Transactions on Neural Networks*, vol. 15, no. 3, pp. 693–701, 2004.

[45] J. Ma, S. S. Ge, Z. Zheng, and D. Hu, "Adaptive NN control of a class of nonlinear systems with asymmetric saturation actuators," *IEEE Transactions on Neural Networks and Learning Systems*, vol. 26, no. 7, pp. 1532–1538, 2014.

[46] J. Wei, Y.-J. Liu, H. Chen, and L. Liu, "Adaptive neural control of connected vehicular platoons with actuator faults and constraints," *IEEE Transactions on Intelligent Vehicles*, 2023. Doi: 10.1109/TIV.2023.3263843.

[47] Y. Li, S. Dong, K. Li, and S. Tong, "Fuzzy adaptive fault tolerant time-varying formation control for nonholonomic multirobot systems with range constraints," *IEEE Transactions on Intelligent Vehicles*, 2023. Doi: 10.1109/TIV.2023.3264800.

[48] F. Falahatraftar, S. Pierre, and S. Chamberland, "An intelligent congestion avoidance mechanism based on generalized regression neural network for heterogeneous vehicular networks," *IEEE Transactions on Intelligent Vehicles*, vol. 8, no. 4, pp. 3106–3118, 2023.

[49] Z. Wang, Y. Zou, Y. Liu, and Z. Meng, "Distributed control algorithm for leader–follower formation tracking of multiple quadrotors: theory and experiment," *IEEE/ASME Transactions on Mechatronics*, vol. 26, no. 2, pp. 1095–1105, 2020.

[50] K. McGuire, C. De Wagter, K. Tuyls, H. Kappen, and G. C. de Croon, "Minimal navigation solution for a swarm of tiny flying robots to explore an unknown environment," *Science Robotics*, vol. 4, no. 35, pp. 9710–9724, 2019.

[51] Y. Zhang, B. Tian, and H. Chen, "Ultra-wideband and visual odometry based relative localization for multi-UAV system," in *Proc. Chinese Control Conference*, pp. 4665–4670, 2020.

[52] G. Loianno and V. Kumar, "Cooperative transportation using small quadrotors using monocular vision and inertial sensing," *IEEE Robotics and Automation Letters*, vol. 3, no. 2, pp. 680–687, 2017.

[53] Y. Huang, W. Liu, B. Li, Y. Yang, and B. Xiao, "Finite-time formation tracking control with collision avoidance for quadrotor UAVs," *Journal of the Franklin Institute*, vol. 357, no. 7, pp. 4034–4058, 2020.

Zhongjun Hu received the B.Eng. degree in automation from the college of information engineering, Zhejiang University of Technology, Hangzhou, China, in 2018, and the M.S. degree in electrical and computer engineering from the Ohio State University, Columbus, OH, USA, in 2020. Since August 2021, he has been working toward a Ph.D. degree with the Department of Mechanical & Aerospace Engineering, University of Kentucky, Lexington, KY, USA.

His research interests include adaptive control and its application of multi-agent systems.

Xu Jin (S'12–M'19) received the Bachelor of Engineering (BEng) degree in electrical and computer engineering (First Hons.) from the National University of Singapore, Singapore, the Master of Applied Science (MASc) degree in electrical and computer engineering from the University of Toronto, Toronto, ON, Canada, the Master of Science (MS) degree in mathematics from the Georgia Institute of Technology, Atlanta, GA, USA, and the Doctor of Philosophy (PhD) degree in aerospace engineering from the Georgia Institute of Technology, Atlanta, GA, USA.

Dr. Jin is currently an Assistant Professor with the Department of Mechanical & Aerospace Engineering, University of Kentucky, Lexington, KY, USA. His current research interests include adaptive and iterative learning control with applications to intelligent vehicles, autonomous robots, and nonlinear multiagent systems.